

长石显微变形机制研究进展

巴合达尔·巴勒塔别克¹⁾, 赵中宝^{2,3)}, 王根厚¹⁾, 孙丽静¹⁾, 赵鹏彬^{1,4)}

1) 地球科学与资源学院, 中国地质大学(北京), 北京, 100083;

2) 自然资源部深地动力学重点实验室, 北京, 100037; 3) 中国地质科学院地质研究所, 北京, 100037;

4) 陕西省矿产地质调查中心, 西安, 710068

内容提要:岩石的变形机制研究一直以来都是构造地质学研究的主题,特别是基于矿物变形的显微构造研究是流变学研究的基础。从近地表到下地壳,岩石的变形从脆性破裂逐渐过渡至韧性蠕变,这些变形过程会被记录在岩石中,形成相应的显微构造。一般来讲,从低温低压至高温高压的变形环境,单一矿物的显微变形机制经历从微破裂、到矿物的溶解-沉淀、到位错蠕变、到动态重结晶作用、到颗粒边界滑移或扩散蠕变等的连续转变,它们之间的转换往往是过渡并且相互影响的,通常也会耦合发生。长石是地壳中含量最丰富的造岩矿物,因此长石的变形行为会直接影响地壳的流变学性质,研究长石的显微变形机制对理解地壳流变学特性至关重要。长石还是一种非常特别的矿物,主要分为斜长石和碱性长石两个端元,由于它们所属晶系的不同,有着差异的变形行为,然而这两个系列的长石在一定的温压条件下又是可以相互转化的,这些物理差异性和化学行为的复杂性造就了长石非常复杂的显微变形特性。本综述从岩石的显微变形机制讲起,随后概述了长石的显微变形特征,尝试归纳不同温度条件下长石的显微变形表现,对比斜长石和钾长石的异同,总结不同显微变形机制对长石结晶学优选方位的影响,最后简单介绍一下国际上显微变形研究方法和技术的进展。

关键词:显微变形机制;长石显微变形;斜长石;钾长石;结晶学优选方位(CPO)

构造地质学的核心是研究地壳的应力与应变,通常在上地壳发生脆性变形(地震带),在下地壳及以下的地幔发生韧性变形(无震或少震带),脆性变形和韧性变形之间发育脆韧性变形过渡带(Goetze et al., 1979; Ramsay, 1980)。脆性变形导致破裂,形成断层,遵循摩尔-库伦破裂准则(Kirby, 1983; Carter et al., 1987),而韧性变形则使岩石发生流变,据此建立起了大家所熟悉的“圣诞树型”地壳流变学模型(Regenauer-Lieb et al., 2003; Bürgmann et al., 2008)。如此复杂形变的研究,主要是基于观测自然界发生变形岩石的显微构造,再开展室内实验岩石学模拟,用模拟的结果去对比天然的显微变形现象,这些都是研究岩石流变学属性的基础(Uenishi, 2009)。因此,流变学的研究基础

是岩石的变形观察及其形成机制研究。

早期的岩石变形研究集中在单矿物上,这样就形成了一系列稳态变形的研究成果(Hirth et al., 2003; Austin et al., 2009)。然而自然界中岩石的变形,往往是具不同流变学性质的矿物共同发生变形的结果,例如在糜棱岩中通常可见连续变形的石英及破碎的长石(例如书斜构造),这代表了两种矿物在相同的变形温压条件下呈现出不同的变形表现,即非稳态变形(Trepmann et al., 2003; Ellis et al., 2004; Qin Xuping et al., 2018)。非稳态变形可能是引发下地壳地震的主要机制(Ellsworth et al., 2005; Shelly, 2010)。研究非稳态变形的前提是把变形体系内不同单矿物的形变特征研究清楚,对单矿物石英的研究开展的很多(Herwegh et al.,

注:本文为西藏荣玛乡南1:5万区域地质调查(编号121201103000150004),中国博士后科学基金(编号2016M601084),陕西省公益性地质项目(编号20170102)联合资助。

收稿日期:2019-07-04;改回日期:2019-08-15;网络发表日期:2019-08-22;责任编辑:黄敏。

作者简介:巴合达尔·巴勒塔别克,男,1989年生。构造地质学在读硕士研究生,Email:answer-180@163.com。通讯作者:赵中宝,男,1985年生,构造地质学博士,中国地质科学院地质研究所助理研究员,长期从事青藏高原羌塘地体地质填图及构造研究。Email:zhaozhb04@163.com。

引用本文:巴合达尔·巴勒塔别克,赵中宝,王根厚,孙丽静,赵鹏彬. 2019. 长石显微变形机制研究进展. 地质学报, 93(10):2678~2697, doi: 10.19762/j.cnki.dizhixuebao.2019250.
Baletabieke Bahedaer, Zhao Zhongbao, Wang Genhou, Sun Lijing, Zhao Pengbin. 2019. Research advances of microstructural deformation mechanism of feldspar. Acta Geologica Sinica, 93(10): 2678~2697.

2011; Hunter et al., 2018), 利用石英显微组构分析剪切带构造变形特征的实例也较常见 (Li Hailong et al., 2017), 但对地壳中另一种常见矿物——长石的变形研究则相对较少, 这可能是由于长石的显微变形机制过于复杂所致。

长石是地壳中含量最丰富的矿物 (Tullis, 2002), 具体可分为斜长石和钾长石两大类, 它们在中下地壳普遍发育, 其显微变形机制严重影响着地壳的流变学属性 (Menegon et al., 2012; Fukuda et al., 2013; Miranda et al., 2016), 例如地震破裂发生的深度、是否在加厚的下地壳存在地壳流及下地壳的渗透率如何等 (Beaumont et al., 2006; Ingebritsen et al., 2010)。不同类型的长石发育不同类型的双晶, 并且化学性质也有较大差异 (常丽华等, 2006), 在一定的温压条件下, 它们可以相互转化, 这导致了长石变形机制的复杂性。因而对主要长石类型的变形机制进行总结分类, 以便我们深入理解长石的变形过程, 也可为中下地壳流变学属性的研究提供一些新的线索。

本综述先从矿物的基本变形机制切入, 给出目前常见的各种变形机制的定义和表现, 接着阐述了不同变形机制发生的原因, 以及它们之间可能的相互关系。第二部分阐述了长石在温度升高条件下其显微变形机制的转化, 介绍了多种变形机制耦合发生的情形。最后本文简单的介绍了目前显微变形研究方法及手段的进展, 方便我们进一步开展相关研究。

1 矿物显微变形机制

矿物的显微变形机制非常复杂, 多数情况下, 多个显微变形机制往往是耦合发生并相互影响的, 它们之间的转换往往是过渡的。本部分尝试从以下几个方面来阐述岩石矿物的显微变形机制。

1.1 矿物的脆性破裂

脆性破裂在矿物中最常见的现象是微破裂。微破裂 (micro-cracks) 是指岩石中矿物颗粒尺度或更小尺度的不连续面, 通常伴随轻微的扩张和位移, 在具各向异性的矿物中, 微破裂通常沿特定的结晶学方向 (如解理面方向) 发育及扩展 (Passchier et al., 2005)。微破裂可能发生在晶格或微裂隙中, 晶体中的流体、固体包裹体中, 或颗粒边界 (Tapponnier et al., 1976)。

微破裂形成的因素很多, 差应力是导致微破裂最重要的一种因素。在含孔隙岩石等不连续介质

中, 微破裂是由于静岩压力造成的孔隙塌陷形成的 (Passchier et al., 2005)。不同矿物间弹塑性的不匹配也可能造成微破裂的生长和扩张 (Hippertt, 1994)。此外, 变形双晶或膝折 (Carter et al., 1978); 热膨胀差异导致相邻矿物的差异收缩 (Vollbrecht et al., 1991); 矿物相转变导致的体积变化 (Kirby et al., 1993) 等因素都会造成微破裂。微破裂通常被二相矿物填充并愈合, 因此不易被观察到, 利用流体包裹体的痕迹或者阴极射线照射等手段能观察到破裂愈合的痕迹 (Stel, 1981)。

1.2 矿物的溶解—沉淀

在岩石变形过程中, 由于高差应力和晶体颗粒边界流体相的影响, 晶体颗粒会发生溶解, 即压溶作用 (pressure solution), 它可以在矿物颗粒没有内部变形的情况下改变颗粒的形状 (图 1) (Passchier et al., 2005)。压溶作用可能出现在矿物颗粒接触面或颗粒间的流体薄膜中 (Rutter, 1976), 也可能出现在“岛型构造”的溶解凹槽中 (Lehner, 1995)。通常压溶作用较慢, 可能无法调节更快的应变速率, 尤其在扩散通道较远的情况下 (如缝合线) (Gratier et al., 1999), 这时造成矿物变形的通常是脆性变形; 在低级变质条件下, 压溶作用和脆性破裂会同时出现 (Passchier et al., 2005)。溶解物质从高浓度区域扩散至低浓度区域, 即溶解扩散 (solution transfer), 溶解物质可能沉淀在颗粒间或

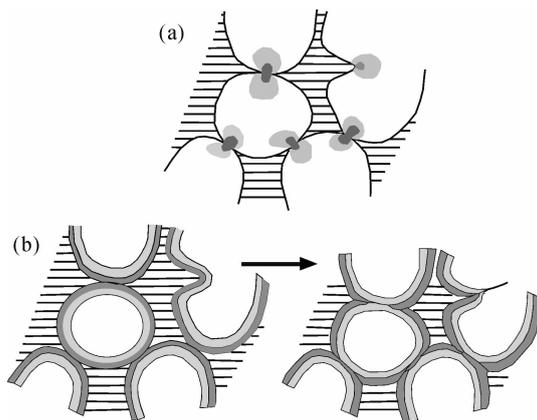


图 1 压溶作用示意图 (Passchier et al., 2005)

Fig. 1 Schematic diagram of pressure solution (Passchier et al., 2005)

(a) — 颗粒被孔隙流体包围, 在颗粒接触点, 差应力相对较高; (b) — 颗粒接触区域溶解的物质会沉淀在邻近的孔隙, 改变颗粒形状
(a) — Oolites surrounded by a pore fluid. At contact points, differential stresses are relatively high; (b) — material dissolved at the contact points is redeposited in adjacent pore spaces and changes the shape of the grains

流体接触区域,也可能迁移较远距离形成细脉或应变压力影 (Passchier et al., 2005)。

溶解—沉淀蠕变 (dissolution-precipitation creep),也称应力诱导的溶解扩散 (stress-induced solution transfer),特指在高正应力区域溶解的矿物颗粒沿晶间流体通道迁移至较低正应力区域并沉淀的变形过程 (Vernon, 2004)。晶界和颗粒表面的粗糙形态被认为是局部溶液—沉淀蠕变的证据 (Mancktelow et al., 2004)。溶解—沉淀过程,与溶解、反应、沉淀、交代、颗粒边界迁移等有关,有时可能是这些过程的特定组合 (Fukuda et al., 2013)。因此,压溶作用、溶解扩散、溶解—沉淀蠕变统称为溶解—沉淀过程。

在富流体的成岩作用至低级变质条件下,溶解—沉淀过程更高效 (Hippertt, 1994; Passchier et al., 2005),在更高的变形变质条件下,压溶作用可能是主导变形机制 (Bell et al., 1989; Wintsch et al., 2002)。在流体含量较低 (<1%)的中地壳环境,很多造岩矿物的变形机制会从位错蠕变转变为溶解—沉淀蠕变 (Tullis et al., 1996; Wintsch et al., 2002),甚至在角闪岩相条件 (Berger et al., 1996; Wintsch et al., 2002)和岩石深熔作用期间 (Álvarez-Valero et al., 2005),溶解—沉淀蠕变也很重要。借助于颗粒边界流体,矿物的溶解—沉淀过程可能是引起地壳中岩石变形的机制 (如溶解—沉淀蠕变: Menegon et al., 2008; Brander et al., 2012; Fukuda et al., 2012)。

1.3 晶体变形

岩石韧性变形很大程度上是通过晶格缺陷的迁移实现的,在没有脆性破裂的情况下,移动的晶格缺陷会造成晶体内部变形,即晶内变形作用 (intracrystalline deformation),晶格缺陷分为点缺陷和线缺陷 (即位错):点缺陷由原子缺失 (vacancy) 或间隙额外原子 (interstitial) 造成;位错是晶体结构插入了额外的半晶格面造成的,分为刃型位错和螺旋位错 (图 2) (Passchier et al., 2005)。

单列位错滑移形成的晶内变形即位错滑移 (dislocation glide);通过迁移位错或空位形成位错线的方式,能有效迁移位错,使位错“越过”障碍物,这类位错迁移配合位错攀移 (dislocation climb),将位错“越过”障碍物的变形机制即位错蠕变 (dislocation creep),位错蠕变使岩石发生韧性变形;通过位错蠕变实现的晶内变形即晶体塑性变形 (crystal plastic deformation) (Passchier et al.,

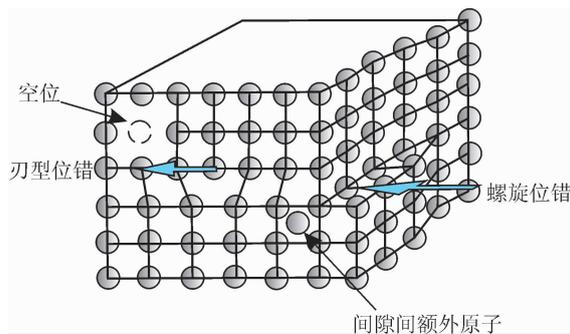


图 2 晶格缺陷及其空间关系 (Andrew, 2015)

Fig. 2 Lattice defects and their spatial relationships (Andrew, 2015)

位错在滑移面上沿着伯格向量定义的方向移动,位错线垂直于伯格向量被称为刃型位错,平行于伯格向量被称为螺旋位错 Dislocations move on slip planes in a direction defined by a vector known as the Burgers vector. Where a dislocation line is perpendicular to the Burgers vector it is called an edge dislocation, while screw dislocations are parallel to the Burgers vector

2005)。因为不同滑移系的相交,有时晶体内的位错不能有效迁移,出现堵塞、缠结,导致应变硬化 (strain hardening),它使岩石更易脆性破裂 (Passchier et al., 2005)。

变形双晶 (deformation twinning) 也会造成矿物的变形 (Egydio-Silva et al., 1999),通常出现在较低温度的形变和特定晶体学方向上 (Passchier et al., 2005)。变形双晶通常呈楔形或平板状,温度升高时,双晶边界会发生膨凸作用,即双晶边界迁移重结晶作用 (twin boundary migration recrystallisation) (图 3) (Rutter, 1995),它与动态重结晶作用的区别在于它不会影响颗粒边界 (Passchier et al., 2005)。膝折与双晶类似,它在单一滑移系的晶体中很普遍,在低温条件下也会出现在石英、长石等矿物中 (Nishikawa et al., 2000; Passchier et al., 2005)。

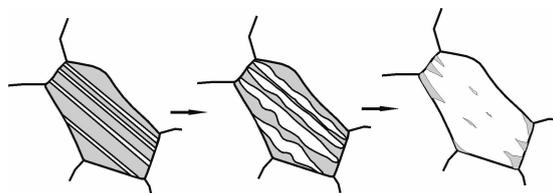


图 3 双晶边界迁移重结晶作用示意图

(Passchier et al., 2005)

Fig. 3 Schematic diagram of twin boundary migration recrystallisation (Passchier et al., 2005)

1.4 动态重结晶作用

因为相邻变形晶体存在位错密度差和自由能

差,变形量较小的晶体会向变形量较大的晶体生长,造成相同矿物中晶体取向、大小和形状的改变,并伴随物质重组,即重结晶作用 (Recrystallisation) (Hirth et al., 1992)。随着温度升高,差应力下降,重结晶作用可依次分为:膨凸重结晶作用、亚颗粒旋转重结晶作用和高温颗粒边界迁移重结晶作用 (Hirth et al., 1992; Lafrance et al., 1996; Stipp et al., 2002),它们是逐渐过渡的,在某些条件下会同时发生 (Lloyd et al., 1994),它们造成晶体的主动变形,被称为动态重结晶 (Dynamic Recrystallisation)。在矿物的持续变形过程中,位错产生和消失是相互竞争的,位错总量会朝平衡状态发展,这种位错密度减少的过程即恢复作用 (Recovery) (图 4),它是形成亚颗粒的主要过程 (Passchier et al., 2005)。

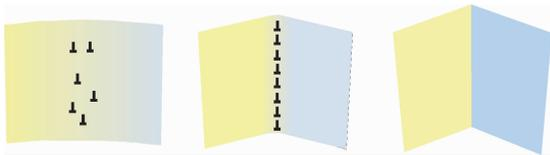


图 4 恢复作用示意图 (Andrew, 2015)

Fig. 4 Schematic diagram of Recovery (Andrew, 2015)

位错堆积在亚颗粒边界造成亚颗粒旋转,在此期间晶体方位的转变逐步明显 (颜色代表晶体方位)

Subgrain rotation caused by the stacking of dislocations into a subgrain boundary, Colour represents orientation where the transition in orientation becomes progressively more distinct during subgrain rotation

1.4.1 膨凸重结晶作用

在低温、高应变率条件下,晶粒边界从低位错密度膨凸到高位错密度形成新晶体即膨凸重结晶作用 (bulging recrystallisation; BLG) (图 5a),它普遍造成核幔构造 (Shigematsu, 1999; Stipp et al., 2002)。BLG 通常沿着母颗粒边界和三联点出现,母颗粒边界不规则,呈叶状突起,部分突起会形成新颗粒,母颗粒通常发生波状消光、膝折、变形纹等 (Passchier et al., 2005)。

1.4.2 亚颗粒旋转重结晶作用

恢复作用形成的亚颗粒通过旋转形成新颗粒即亚颗粒旋转重结晶作用 (subgrain rotation recrystallisation; SGR) (图 5b),SGR 通常使母颗粒发生韧性变形,普遍发育波状消光,新老颗粒间过渡不明显,亚颗粒也被轻微拉长,从亚颗粒边界至颗粒边界有渐变过渡带 (Passchier et al., 2005)。

1.4.3 高温颗粒边界迁移重结晶作用

在高温、低应变率条件下,颗粒边界迁移活跃到某种程度以至于颗粒边界能横扫整个晶体来移除位错和可能存在的亚颗粒边界,即高温颗粒边界迁移重结晶作用 (high-temperature grain boundary migration recrystallisation; GMB) (图 5c) (Stipp et al., 2002; Passchier et al., 2005)。GMB 造成较大的颗粒粒径差异,新生大颗粒有朵间状至变形虫状颗粒边界 (图 6),如果集合体中有二相矿物,会发育牵引构造、窗户构造、拖拽构造,在二相矿物被完全交代前,可能出现它的残余颗粒 (图 7) (Passchier et al., 2005)。在长石、角闪石等固溶相矿物中,BLG 和 GMB 不仅被内部应变能驱动 (Passchier et al., 2005),也被新老颗粒中不同化学成分驱动 (Berger et al., 1996; Stünitz, 1998)。

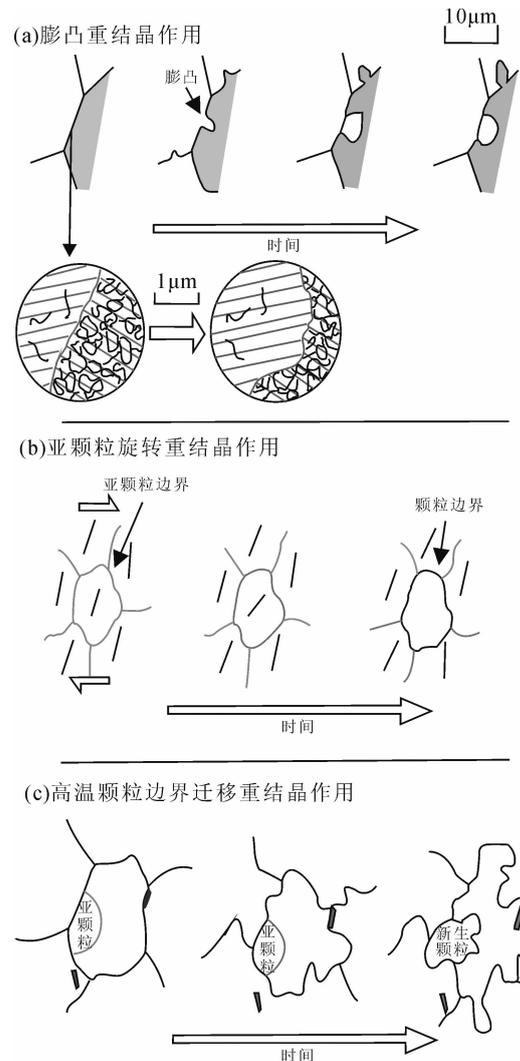


图 5 动态重结晶作用示意图 (Passchier et al., 2005)

Fig. 5 Schematic diagram of Dynamic Recrystallisation (Passchier et al., 2005)

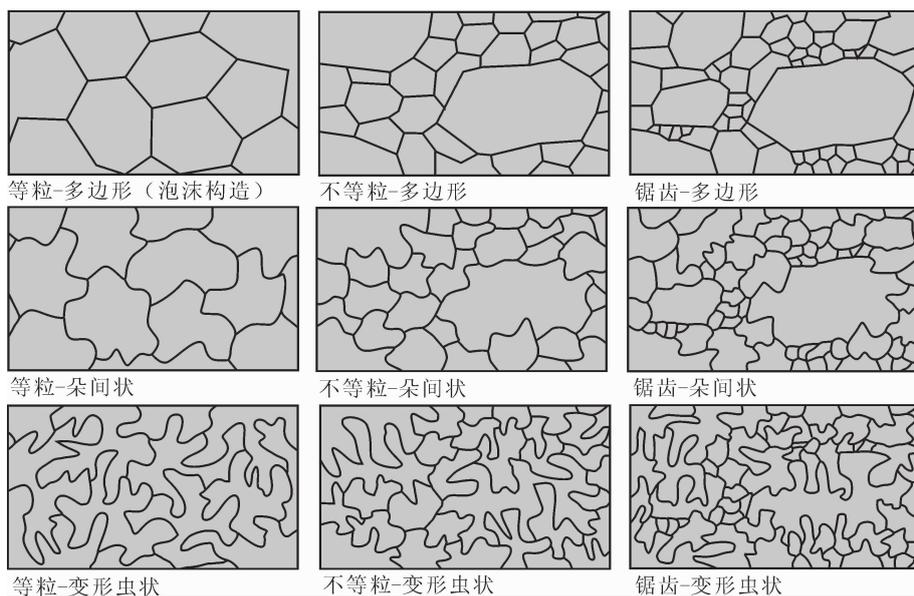


图6 朵间状等颗粒边界示意图 (Passchier et al., 2005)

Fig. 6 Schematic diagram of interlobate grain boundary shape etc. (Passchier et al., 2005)

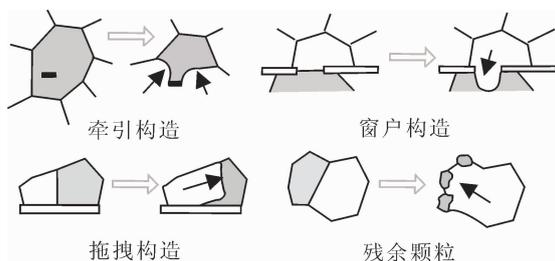


图7 牵引构造等示意图 (Passchier et al., 2005)

Fig. 7 Schematic diagram of pinning microstructure etc (Passchier et al., 2005)

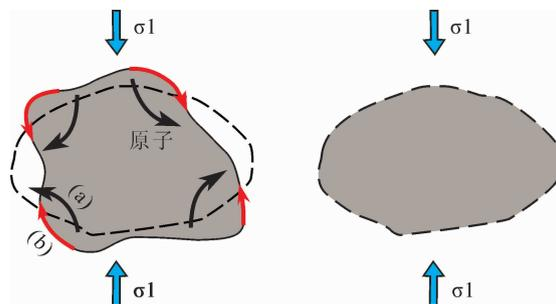


图8 物质扩散蠕变 (Andrew, 2015)

Fig. 8 Schematic diagram of diffusive mass transfer (Andrew, 2015)

原子通过两种方式从高应力区域扩散至低应力区域:

(a)—Nabarro-Herring 蠕变, (b)—Coble 蠕变

Atoms diffuse from high to low stress regions by two ways:

(a)—Nabarro-Herring creep, (b)—Coble creep

1.5 扩散蠕变和颗粒边界滑移

当变形岩石的温度接近熔融温度时,晶格缺陷会以穿越晶格的方式使晶体发生变形,即晶体尺度物质扩散迁移 (grain-scale diffusive mass transfer) (Passchier et al., 2005)。它包括 Coble 蠕变和 Nabarro-Herring 蠕变,前者指晶格中的缺陷沿晶体边界扩散,后者指扩散的缺陷会穿越晶体 (图 8) (Knipe, 1989; Wheeler, 1992)。

通过物质固态的扩散迁移,使晶体局部塑性变形增强或以颗粒边界流体的溶解和沉淀等来防止颗粒间孔隙的发展,即颗粒流变形 (granular flow) (Paterson, 1995; Fliervoet et al., 1997)。在特高应力环境,变形的等轴细粒集合体不会形成明显的 CPO (结晶学优选方位) 或 SPO (形态优选方位) 的现象,即超塑性 (superplasticity) (Boullier et al., 1998b)。Coble 蠕变、Nabarro-Herring 蠕变、颗粒流变形和超塑性的流变学规律非常相似,因此

将它们统称为扩散蠕变 (diffusion creep) (Passchier et al., 2005)。在高级变质条件下,扩散蠕变可能在不同矿物间产生强烈弯曲和叶状的颗粒边界 (Gower et al., 1992)。

晶体间相对滑移即颗粒边界滑移 (grain boundary sliding; GBS),在细粒集合体中尤其明显 (Passchier et al., 2005),为预防颗粒边界的空隙扩大,颗粒间必须相互滑移以形成相对稳定的组构 (图 9) (Andrew, 2015)。如果细粒矿物集合体经历高应变后,缺乏明显的 CPO,且由等轴颗粒组成,或 CPO 不能被位错活动所解释,则可间接说明其主要变形机制是 GBS (Fliervoet et al., 1997;

Bestmann et al., 2003), 此外, 低应变区至高应变区晶界角度逐渐升高 (Jiang et al., 2000); 晶体取向差轴的随机化 (Jiang et al., 2000; Bestmann et al., 2003); 由机械混合或异相成核造成的相混合 (Warren et al., 2006; Dimanov et al., 2007) 等能作为 GBS 的证据。需要注意的是, CPO 的存在不能被作为证据来否定 GBS (Rutter et al. 1994; Berger et al. 1996)。实验岩石学的研究表明 GBS 能被许多过程调节 (Mukherjee et al., 1996; Wakai et al., 1999), 较常见的是位错蠕变调节的颗粒边界滑移 (dislocation-accommodated grain boundary sliding; DisGBS), 它是位错蠕变和扩散蠕变之间的过渡机制, 会造成中等 CPO 和弱 SPO (Svahnberg et al., 2010)。

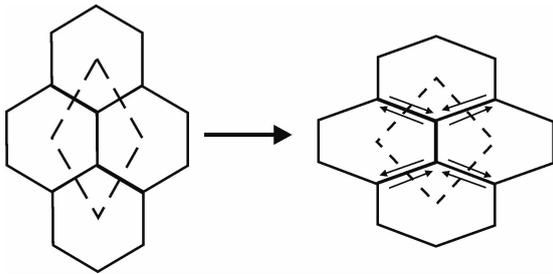


图 9 物质扩散迁移被颗粒边界滑移调节 (Andrew, 2015)
Fig. 9 Diffusional mass transport accommodated by grain boundary sliding (Andrew, 2015)

此外, 有学者提出在 GBS 的驱动下, 会形成晶内破裂, 即空洞化作用 (Cavitation): 在 GBS 影响下, 扩散的空位会在张力较大的晶界 (σ_3 的方向) 成核, 随后在张力较小的晶界聚集形成晶间空洞, 受其影响, 塑性变形局限在“桥”(未受损的晶界), 当“桥”失去稳定性局部收缩时, 便会形成晶内破裂 (Vollbrecht et al., 1999; Kassner et al., 2003; Zavada et al., 2007); 位错堆积在晶格杂质中或堆积在晶界 (Zener-Stroh 牵制机制) 也能造成界内破裂 (图 10)。

1.6 颗粒表面积减少引发的静态重结晶作用

岩石变形过程中, 矿物颗粒表面积的减少会降低内部自由能 (Kruhl, 2001; Evans et al., 2001), 因此多晶体矿物集合体更倾向于形成多边形、大粒径的颗粒组构, 这种颗粒边界迁移造成颗粒生长、边界变平直的过程即颗粒表面积减少 (grain boundary area reduction; GBAR) (图 11), 变形停止后, GBAR 可能占主导地位, 在高温条件下尤其明显; GBAR 会促使单矿物集合体形成泡沫构造 (foam-

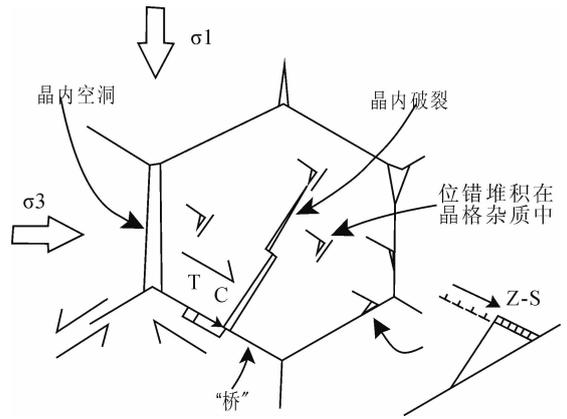


图 10 空洞化作用示意图 (Zavada et al., 2007)
Fig. 10 Schematic diagram of Cavitation (Zavada et al., 2007)

T 和 C 表示晶界边缘的拉伸和压缩部分。Z-S 表示空洞形成的 Zener-Stroh 牵制机制
T and C designate the tensional and compressive sector of a grain boundary ledge. Z-S designates illustration of the Zener-Stroh mechanism of cavity formation

structure) (图 6), 因为强各向异性的影响, 多矿物集合体不易形成泡沫构造 (Passchier et al., 2005)。由 GBAR 造成的矿物粒径大小不仅取决于变形温度, 更取决于存在于颗粒边界的固相、液相以及矿物化学成分和 CPO 的变化, 所以, 在 GBAR 的影响下, 若成层较厚、矿物成分单一, 则形成较大的颗粒, 若成层较薄或矿物成分复杂, 则形成较小的颗粒, 这被称为 Zener 牵制作用 (Zener pinning) (Evans et al., 2001; Krabbendam et al., 2003)。岩石停止变形后, 在温度相对高或颗粒边界含水时, 恢复作用、动态重结晶作用和 GBAR 可以继续发展, 即静态重结晶作用 (Static Recrystallisation) (Evans et al., 2001; Passchier et al., 2005), 它会消除波状消光和亚颗粒, 破坏 SPO, 不稳定矿物被稳定矿物取代, 颗粒变大边界变平直 (Passchier et al., 2005)。尽管如此, 部分颗粒的核部仍可能不受静态重结晶作用的影响, 保留原始颗粒的尺寸、形

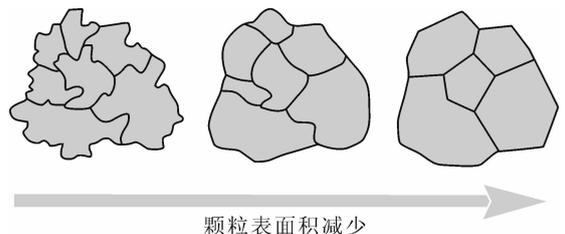


图 11 颗粒表面积减少示意图 (Passchier et al., 2005)
Fig. 11 Schematic diagram of grain boundary area reduction (Passchier et al., 2005)

状和化学成分 (Jessell et al., 2003)。

1.7 各种显微变形机制之间的相互联系

变形岩石中任何变形阶段和最终表现都取决于应变速率及应变过程所处的温度等因素,比如高温环境和颗粒边界流体会促进静态重结晶作用;或在高温环境和高差应力条件下,扩散蠕变可能伴随或取代位错攀移和重结晶作用 (Passchier et al., 2005)。本章节将试图列举几个机制之间的相互转换。

破裂,溶解—沉积,扩散蠕变之间是相互联系的。高温高压变形实验显示微裂缝产生膨胀,微裂缝周围的局部压力会下降,从而促进熔体形成 (Negrini et al. 2014),而熔融体的存在会促进颗粒边界的运输速率,进而增强交代和溶解—沉淀蠕变 (Tullis et al., 1996; Hirth et al., 2003)。中上地壳广泛分布的石英和长石 (Vernooij et al., 2006),因为溶解—沉淀蠕变的影响,形成细晶粒,进而促进GBS和扩散蠕变 (Wintsch et al., 2002; Kenis et al., 2005; Menegon et al., 2008)。岩石中广泛发育的破裂也会促使颗粒粒径减小及流体渗透,促进GBS (Menegon et al., 2008; 2013)。存在部分熔融的情况下,较高的应变速率有利于扩散蠕变的发生 (Hirth et al., 1995),而应变速率的增加不仅取决于熔融体的粘度 (Cooper et al., 1984),也取决于颗粒边界的湿度 (Hirth et al., 1995; Dimanov et al., 2000)。Fukuda et al. (2012)的研究认为,矿物溶解—沉淀过程中可能会释放水。因此在温度较高、应变较强的条件下,水致破裂会促进溶解—沉淀蠕变和扩散蠕变,而溶解—沉淀蠕变与扩散蠕变也相互促进。

破裂与重结晶作用的联系也极为紧密。通常认为,破裂发生在低级变质条件下,而且下地壳中脆性变形的显微证据可能因为破裂的愈合、颗粒生长熔接等而被消除 (Menegon et al., 2013),但有证据表明即使在塑性变形的高温高压条件下也会发生碎裂作用 (Kenkmann, 2000; Handy et al., 2002)。透射电子显微镜分析表明,破裂是由碎片组成的狭窄区域 (Stünitz et al., 2003; Trepmann et al., 2007),从断裂壁上脱落的碎片可能提供重结晶所需的晶核,减少的表面能和应变能会驱动沿破裂发生GMB (Menegon et al., 2013)。渗透的流体也可能促进沿破裂的GMB,因为流体会显著增强颗粒边界的物质迁移能力 (Mancktelow et al., 2004; Menegon et al., 2013)。

矿物粒径大小对决定变形过程中的应变机制起主导地位。在下地壳剪切带中,动态重结晶作用 (Raimbourg et al., 2008)、矿物反应 (De Ronde et al., 2005; Pearce et al., 2011)和细粒新相矿物的成核 (Küster et al., 1999; Kenkmann et al., 2002)都会导致颗粒粒径减小和矿物多相混合,进而促进扩散蠕变 (Menegon et al., 2013)。如果基质中的颗粒边界由相同矿物构成,则形成严格的单矿物集合体,这可能导致SGR和GMB等 (Menegon et al., 2013);如果颗粒边界由不同矿物构成,认为其变形机制是GBS、扩散蠕变或异质成核作用 (Franek et al., 2011; Kilian et al., 2011; Menegon et al., 2013)。二相矿物的混合会阻碍颗粒生长,所以二相矿物的出现有助于GBS (Küster et al., 1999; Krabbendam et al., 2003)。

造成颗粒粒径减小的变形机制可能有利于应变局部化。应变局部化主要发生在断层和剪切带中 (White et al., 1980),导致应变局部化的主要因素之一是颗粒粒径减小 (Montési et al., 2003),颗粒粒径减小极有可能造成变形机制的转变,使岩石从位错蠕变转变至GBS或扩散蠕变,从而降低剪切带的强度 (Kenkmann et al., 2002; Raimbourg et al., 2008)。

溶体和熔体在岩石变形过程中的作用至关重要。分布在颗粒边界的溶体薄膜会提供高扩散率的通道,促进蠕变速率 (Hirth et al., 1995),而受限在三联点的溶体仅轻微的增强扩散蠕变的速率 (Cooper et al., 1984; Dimanov et al., 1998)。对部分熔融花岗岩集合体的变形实验表明,晶体内少量熔体会增强变形岩石的蠕变速率,随着熔体含量的增加,变形机制会从位错蠕变转变为熔融增强的扩散蠕变 (Dell' Angelo et al., 1987, 1988)。对确定变形期间的固有强度和变形机制而言,熔体的连通性至关重要,在熔体含量约0~7%之间,岩石强度降低了两个数量级 (Rosenberg et al., 2005)。岩石强度的急剧下降与未发生部分熔融的岩石转变成熔融物质形成高度互连网络通道相关,这种现象被称为熔体连通性阈值 (melt connectivity threshold, MCT),在MCT中,存在两种类型的变形行为:在熔体含量很低(1%~4%)的天然岩石和模拟实验中,主要变形机制是颗粒边界迁移伴随位错蠕变 (Dell' Angelo et al., 1988; Walte et al., 2005)。在较高的熔体含量(<8%),局部剪切带中的主要变形机制是GBS,它将熔体引入剪切

带,剪切带的局部膨胀和压实使熔体在变形带内活动,而不是被分离和迁移出去(Walte et al., 2005)。

2 长石显微变形特征

2.1 长石分类

长石是一组含有钾、钠、钙的铝硅酸盐矿物,偶尔也会有钡、铯及这些元素的类质同象成分混入(Heyes et al., 2012)。长石分为斜长石和碱性长石(钾长石)两个系列(图 12),每个长石都是端元成分间的连续固溶体系列,它们的物理性质很相似,大多数呈现两个方向的完全解理,接近或等于 90° (Zhang et al., 2018)。长石具有各向异性的晶体化学特性(Xu et al., 2017),斜长石属三斜晶系,钾长石多数属单斜晶系(图 13)(常丽华等, 2006)。

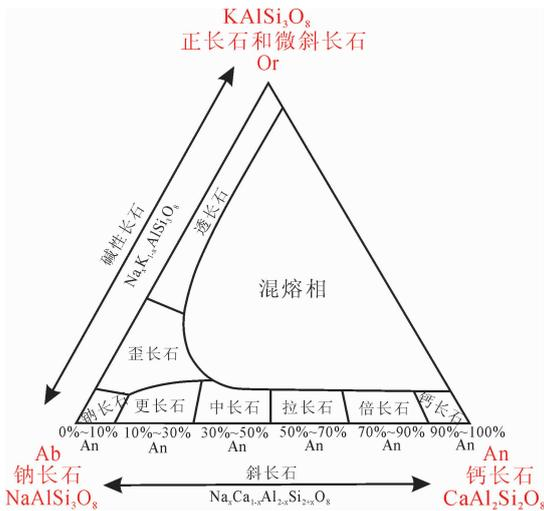


图 12 长石固溶体的不同矿物相图(Zhang et al., 2018)

Fig. 12 Compositional phase diagram of the different minerals that constitute the feldspar solid solution (Zhang et al., 2018)

2.2 长石显微变形机制概述

长石和其它矿物一样,在不同变形条件下其变形表现差别也很大,开展天然长石的显微变形结构研究是理解长石不同变形机制相互作用的主要手段。研究长石的微破裂有利于理解岩石中破裂和高温变形之间的关系(Tullis et al., 1987),如在麻粒岩相条件下,长石中的微破裂可能表明在变形开始时是高差应力环境(Menegon et al., 2013);高温高压实验研究也表明在缺乏高孔隙流体压力条件下,单个长石晶体中的破裂能指示高差应力变形和矿物强度(McLaren et al., 2001; Stünitz et al., 2003)。尽管有证据表明长石在高温条件下也会发生显微破裂,但随着温度升高,长石矿物的位错活动

性和晶体塑性变形会优先于破裂起主导作用(Kruse et al., 2001; Kanagawa et al., 2008; Mehl et al., 2008)。

水含量在矿物变形过程中的作用至关重要。含水流体有助于溶解—沉淀蠕变,但在研究各类长石的变形机制时,对含水流体的推测大多是基于长石周围存在的含水矿物(Ree et al., 2005; Menegon et al., 2006),Fukuda et al. (2012)利用红外光谱技术精细检测了钾长石中水的分布,相比碎斑,细粒钾长石的含水量较低,且均匀分布,这被认为是钾长石溶解—沉淀过程中有少量水被释放,并推测在富水的中地壳环境普遍发生溶解—沉淀蠕变,形成细小的颗粒,进一步促进GBS或扩散蠕变,而它可能弱化和随机化原先形成的较强CPO。

长石在变形过程中是如何细粒化的一直以来都是研究重点,长石发生颗粒粒径的变化会促使变形机制的转变。除破裂、溶解—沉淀蠕变及发生蠕英结构的反应外,动态重结晶也会促使长石颗粒粒径的减小(Ree et al., 2005; Ishii et al., 2007)。在天然变形的斜长石中,SGR和GMB很常见(Ji et al., 1990; LaFrance et al., 1996)。长石中碎斑与重结晶颗粒间的化学反应很普遍(Kenkmann et al., 2002; Franek et al., 2011),这被认为是经典成核作用作为同构造重结晶机制的主要证据(Stünitz, 1998; Kenkmann et al., 2002)。若动态重结晶斜长石呈现明显SPO和弱—中CPO,有低角度亚颗粒边界和双晶,并且细粒基质有应变局部化,这些现象可能是由DisGBS造成的(Svahnberg et al., 2010; Hansen et al., 2011)。随着温度升高,长石的DisGBS会转换为熔体诱导的扩散蠕变和GBS,显著降低岩石强度,这种变形表现在石英位错蠕变控制的重结晶变形中未被发现(Zavada et al., 2007)。如果长石颗粒呈现等体积的多边形、无SPO、弱或无CPO,且达到高有限应变强度,这些证据能指示其变形机制为Dgh-GBS(grain boundary diffusion accommodated grain boundary sliding)(Wadsworth et al., 1999),它可能发生在部分熔融参与的自然条件下(Dell'Angelo et al., 1987)。

长石还存在一种特殊的矿物类型——条纹长石,它由钾长石和钠斜长石共同组成,同时呈现钾长石和钠斜长石的脱溶结构,它的重结晶作用会造成两相长石的融合,促使应变局部化,条纹长石碎斑的粒径可能受两相长石融合的牵制,若颗粒粒径保持

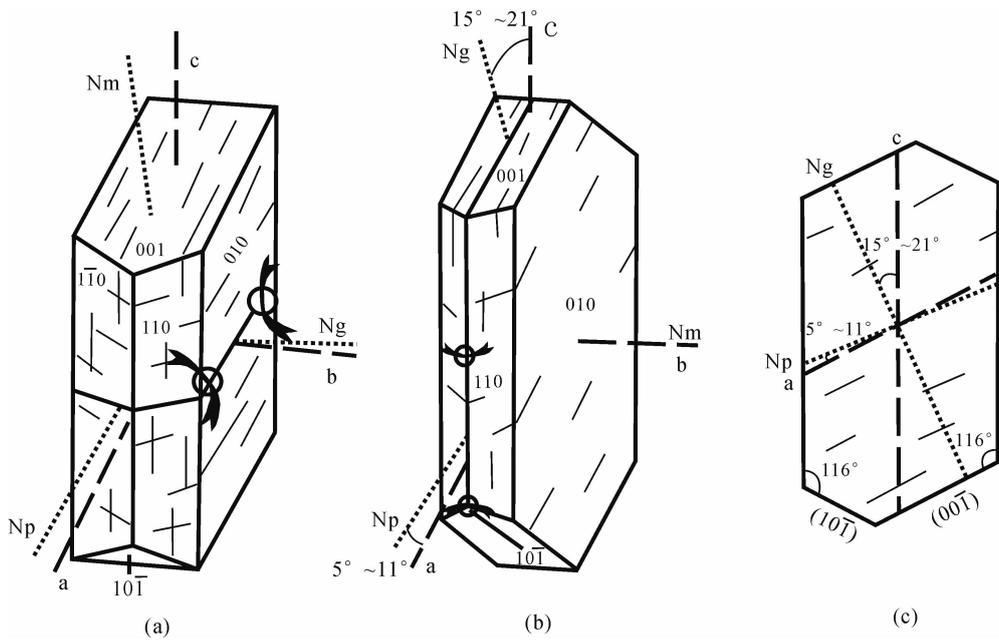


图 13 斜长石和钾长石晶体形态

Fig. 13 Crystal morphology of Plagioclase and K-feldspar

(a)—更长石光性方位图; (b)—透长石光性方位图; (c)—透长石平行(010)切面图(常丽华等, 2006)

(a)—optical orientation diagram of oligoclase; (b)—optical orientation diagram of Sanidine

(c)—sanidine parallel (010) cutaway

在足够小的尺度, 扩散蠕变优先于位错蠕变, 成为主要的变形机制 (Mehl et al., 2008; Kanagawa et al., 2008; Menegon et al., 2013)。因此, 在下地壳富细粒条纹长石的麻粒岩中, 扩散蠕变可能是主要变形机制, 伴随 GBS 和异质成核, 造成糜棱剪切带明显的强度弱化和应变集中, 条纹长石中普遍发育的两相长石边界或许能作为一个显微构造证据来指示这些变形机制。此外, 二长糜棱岩中条纹长石颗粒的重结晶作用总是与破裂的初始阶段一起发生, 可能因为晶体内极低的含水量, 高强度的条纹长石在变形的起始阶段不能进行水解弱化和位错蠕变 (Menegon et al., 2013)。在麻粒岩相条件下, 位错蠕变也是造成条纹长石变形的机制, 还会经历广泛的 SGR, 伴随出溶结构 (Martelat et al., 1999; Franek et al., 2011)。条纹长石的显微构造演化可能会反应从干—强到湿—弱变形环境的过渡 (Menegon et al., 2013)。

2.3 长石在不同温度条件下的显微变形特征

在低级变质条件下 ($<400^{\circ}\text{C}$), 长石变形主要与脆性破裂和碎裂流有关 (如图 14a, 14b)。碎裂形成大小丰富、有棱角的颗粒碎片, 碎片呈现弯曲解理面和双晶等晶内变形, 通常发育不均匀波状消光和边界模糊的亚颗粒 (Tullis et al., 1987)。

Pryer (1993) 认为长石在低温区域普遍发育对立式破裂组合, 在较高温度区域, 发育复合式破裂组合。在天然变形的斜长石中, 细粒黑云母和角闪石的踪迹可以表明破裂在后期愈合, 说明破裂内有局部渗透的流体, 微弱的晶格取向差带也能指示愈合 (Vernon et al., 2004)。钠长石变形双晶和肖钠长石双晶在这个变形阶段很重要 (Egydio-Silva et al., 1999), 钠长石双晶可能在微破裂的顶部形成, 反之亦然 (McLaren et al., 2001)。在较低的温压条件下, 由于长石在 (001) 和 (010) 面发育两组极好的完全解理, 因此破裂可能沿解理面发生 (Tullis et al., 1987)。

在中低级变质条件下 ($400\sim 500^{\circ}\text{C}$), 长石变形仍受微破裂影响, 但受控于少量位错滑移 (Passchier et al., 2005), 由此可能出现条带状变形双晶、弯曲双晶、波状消光、变形带和棱角状膝折带等 (如图 14c) (Pryer, 1993), 出现 BLG (Shigematsu, 1999)。长石普遍发育书斜式微破裂, 破碎的微颗粒通常聚集在被拉长碎颗粒的端部 (Pryer, 1993; Passchier et al., 2005)。在钾长石矿物颗粒中, 尤其颗粒边界的高应力区, 可能出现火焰状条纹长石, 它被认为是斜长石向绢云母的退变质反应过程中引发的钠长石交代钾长石所造成的;

交代过程在晶内变形较强的区域优先发生,如两个长石颗粒接触的部位 (Pryer et al., 1996)。晶内塑性变形逐步成为钾长石内的主导变形机制 (Stunitz et al., 1993; Menegon et al., 2008),位错蠕变也可能被激活 (Menegon et al., 2006)。在绿片岩相环境下,天然变形的花岗质糜棱岩中,Ishii et al. (2007) 认为细粒钾长石的变形由位错蠕变引起,位错蠕变形成强 CPO。

在中级变质条件下 (450~600℃),长石更可能出现位错攀移,重结晶作用逐渐增强,沿颗粒边缘尤其明显 (Passchier et al., 2005)。在此阶段长石主要发生成核作用和新颗粒生长造成的 BLG (Tullis et al., 1991),发育典型核幔构造 (如图 14d) (Passchier et al., 2005)。破裂作用减弱,但普遍发育微膝折,它可能与位错缠结区域的碎裂有关 (Tullis et al., 1987; Altenberger et al., 2000)。如果出现较大的膝折带,它们的边界则不明显 (Pryer, 1993)。GBS 被认为是细粒长石的主要变形机制 (Tullis et al., 1990),但很难通过光学显微镜,甚至透射电镜认定,唯一判断标准是缺乏一致的 CPO 和细粒集合体中长石颗粒与其他颗粒不寻常的均匀混合 (Passchier et al., 2005)。Tullis et al. (1990) 认为,微观断层区域会经历重结晶作用并发育小型韧性剪切带,破坏早先大部分的脆性破裂现象。

在此阶段,钾长石的变形双晶较少发育,钾长石碎斑边缘会发育蠕英结构 (Passchier et al., 2005)。蠕状长石替换钾长石是由晶格扭曲驱使的,这在钾长石各阶段的变形都普遍发生,蠕状长石的形成与颗粒边界流体相中钾长石新颗粒的沉淀有关,在流体 >1% 的地方,会出现蠕状长石交代现象 (如图 14e) (Menegon et al., 2006, 2008)。在低角闪岩相的花岗质糜棱岩中,温度条件能激发位错蠕变时,钾长石的变形由溶解-沉淀蠕变主导,形成弱 CPO (Menegon et al., 2008);斜长石变形过程中,溶解-沉淀作用也较活跃 (如图 14f),重结晶集合体中钠长石颗粒边缘奥长石过度生长造成的不对称性可以指示该现象 (Menegon et al., 2006, 2008)。

在高级变质条件下 (600~700℃),长石更易发生位错攀移和重结晶恢复作用,形成真正的亚颗粒构造 (Küster et al., 1999; Altenberger et al., 2000)。会同时出现 BLG 和 SGR,核幔构造依然存在,但相比在较低温度条件,此时的核幔边界不太明

显;沿解理面普遍发育蠕英结构;在低-中压力条件下,长石颗粒无应变,发育独立的微膝折带,不发育火焰状条纹长石 (Passchier et al., 2005),微破裂现象有时仍很普遍 (Berger et al., 1996; Kruse et al., 2001)。对斜长石而言,在高温半固相条件下,GMB 和位错蠕变共同发生,形成锯齿状或叶片状颗粒边界,矿物颗粒选择性生长,亚颗粒形成,波状消光发育,拉长碎斑发育强 SPO 和 CPO 等显微构造 (Mancktelow et al., 2005; Lund et al., 2006)。

在更高级变质条件下 (>700℃),Rybacki et al. (2004) 的研究认为在 10^{-12} s^{-1} 的地质应变速率下,粒径约 20~30 μm ,流体压力 <10MPa 时,长石颗粒的变形机制主要为扩散蠕变 (如图 14g, 14h)。Menegon et al. (2013) 研究麻粒岩相二长糜棱岩的变形行为后指出扩散蠕变伴随溶解迁移,颗粒(相)边界滑移和异质成核是重结晶长石基质中的主要变形机制。在 900℃,固态长石(钠长石和钾长石)的化学均匀化发生在裂缝和含熔体区域附近,产生可变的中间组分,变形机制主要是溶解-沉淀过程 (Negrini et al., 2014)。

对斜长石而言,在约 700℃、900 MPa 的变质条件下,发生破裂的斜长石发育有两种碎斑:一种为“软”定向,具高长短轴比,易在 (010)[001] 滑移系滑移,主要变形机制是 SGR,它容易形成新颗粒;另外一种为“硬”定向,具较低长短轴比,不易在 (010)[001] 滑移系滑移,普遍发育微破裂,新颗粒通常沿破裂发育,它对动态重结晶期间新颗粒成核起重要作用,因为随后的颗粒边界迁移,颗粒可能生长 (Kruse et al., 2001)。Miranda et al. (2016) 在角闪辉长糜棱岩中的斜长石中观察到位错蠕变过渡至 GisGBS 的显微构造现象,GisGBS 会导致斜长石发生超塑性变形,有利于颗粒保持较小的粒径,促进应变局域化;此外,GisGBS 会形成较强的 SPO、弱 CPO,并启动较多的滑移系。当温度 >850℃时,部分熔融的斜长石中 GMB 广泛发育 (Lafrance et al., 1996; Rosenberg et al., 2003),无应变颗粒、朵间状颗粒边界、残余颗粒等能指示这一过程 (Passchier et al., 2005)。动态重结晶造成晶体变形时,化学成分不会变化 (Guillope et al., 1979),但化学反应可能与动态重结晶同时发生 (Tullis et al., 1991; Stunitz, 1998),斜长石重结晶作用期间的成分变化可能与变形期间的进变质作用和退变质作用有关 (Stunitz, 1998)。在 900℃,1.0GPa 条件下,斜长石通过位错蠕变作用变形 (尽管发生水化

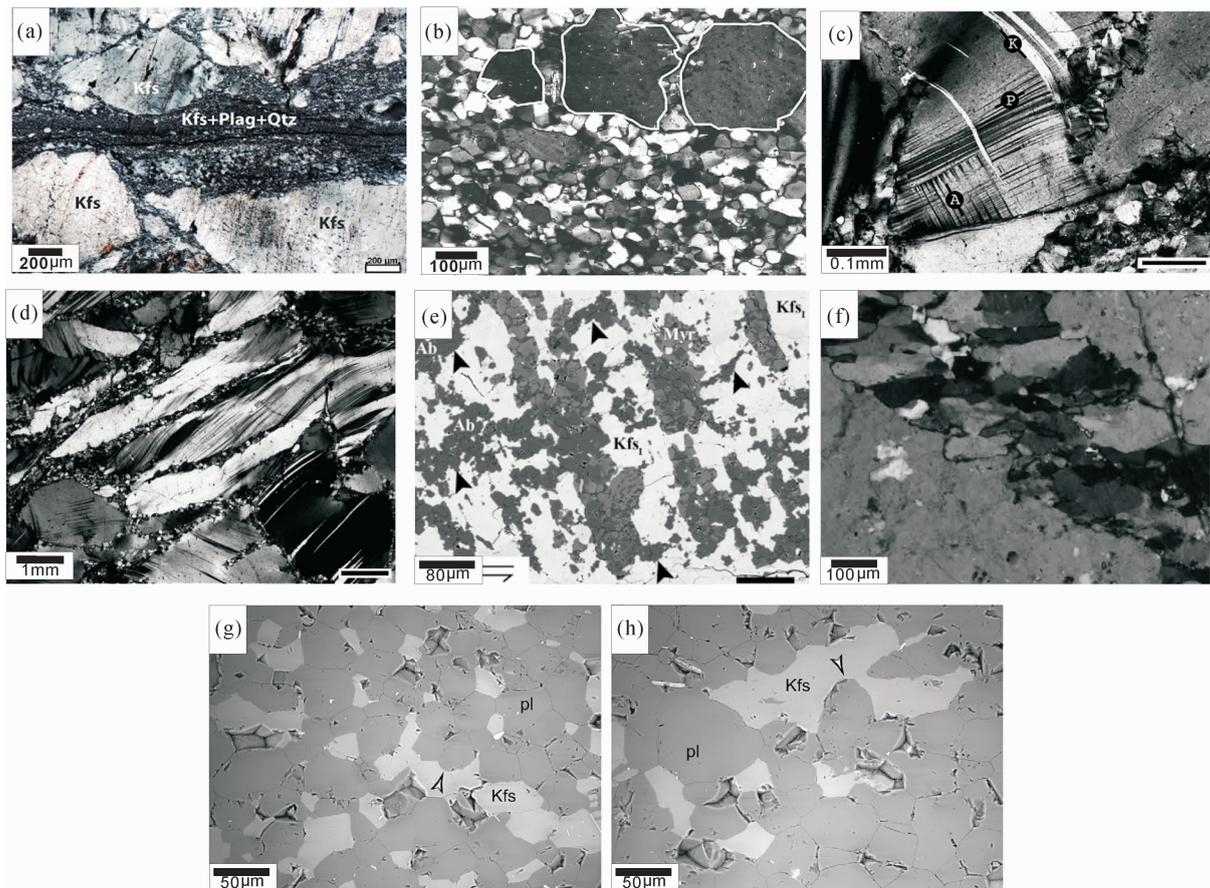


图 14 常见的长石显微构造现象

Fig. 14 Common feldspar microstructures

(a)— C' -type 剪切带中的长石碎斑,石英条带嵌入剪切带中(偏光镜)(Viegas et al., 2016);(b)—一条纹长石的碎斑布丁平行于糜棱岩面理,嵌入重结晶的长石基质中(偏光镜)(Menegon et al., 2013);(c)—斜长石中变形诱导的双晶,钠长石双晶(-A-),肖钠长石双晶(-P-),卡式双晶(-K-)(偏光镜)(Kruse et al., 2001);(d)—膨凸重结晶作用形成的核幔构造,窄带中的重结晶作用横切斜长石碎斑,在没有明显应变的情况下新生拉长的颗粒(偏光镜)(Kruse et al., 2001);(e)—沿钠长石片晶生长的蠕状长石(Myr),它沿正交的片晶组发育较少,如箭头所示(扫描电镜-背散射图像)(Menegon et al., 2006);(f)—拉长的钾长石颗粒沉淀在裂隙中(偏光镜)(Menegon et al., 2008);(g, h)—钾长石和斜长石间的叶状颗粒边界,这类显微构造通常归因于扩散蠕变变形期间的相边界迁移过程,指示物质在颗粒尺度运移(背散射图像)(Menegon et al., 2013)

(a)—Optical micrograph of a C' shear band showing its boundaries with feldspar porphyroclasts, quartz ribbons are embedded in the band (Viegas et al., 2016); (b)—perthite porphyroclast boudinaged parallel to the mylonitic foliation and embedded in the matrix of recrystallized feldspars (crossed polarizer) (Menegon et al., 2013); (c)—deformation-induced twinning in plagioclase; albite twins (-A-), pericline twins (-P-), karlsbad twins (-K-) (light microscopy) (Kruse et al., 2001); (d)—core-mantle structure formed by BLG-recrystallisation. Recrystallisation on narrow bands crosscutting plagioclase porphyroclasts produces new elongated grains without a high amount of strain (light microscopy) (Kruse et al., 2001); (e)—myrmekite (Myr) growing along albite lamellae and it is less developed along the orthogonal set of lamellae (see arrows) (SEM-BSE image) (Menegon et al., 2006); (f)—elongated K-feldspar grains precipitated within a fracture (Crossed polars) (Menegon et al., 2008); (g, h)—lobate phase boundaries between plagioclase and K-feldspar. These microstructures are commonly attributed to phase boundary migration processes during diffusion creep deformation and imply material transport at the granular scale (SEM backscatter electron images) (Menegon et al., 2013)

反应和破裂)(Tullis et al., 1992),相较于钾长石,单个斜长石晶体在同一方向上的变形呈现相似或更高的流动压力(Stünitz et al., 2003)。

对钾长石而言,在 700°C 的温度条件下,它可以以脆性变形机制为主,普遍发育破裂(Holtz et al.,

1992; Johannes et al., 1996)。Negrini et al. (2014)对单个条纹状钾长石晶体和粉末的实验也得出类似结论。例如在应变速率约 10^{-6}s^{-1} 的条件下,在 700°C 和 0.75GPa 时,钾长石的变形由无熔融的脆性剪切破裂主导,而在 900°C 、 0.9GPa 时,变

形主要由同时发生的部分熔融和破裂造成,此时的变形是半脆性的,在 700~900°C 的温度范围内出现脆性至半脆性变形的过渡。此外, Negri et al. (2014) 通过钾长石的变形实验表明,随着流动应力降低和出现熔融,在高温高压条件下的脆性破裂会转变为粘性蠕变,在没有晶体塑性变形的情况下,含粘弹性成分的半脆性变形很可能是扩散蠕变和 GBS (或溶解-沉淀蠕变)。在下地壳的高级正片麻岩中,钾长石集合体的空洞化作用可能形成晶内破裂 (Zavada et al., 2007)。

在超高温的条件下 (950~1200°C, 400MPa), Rybacki et al. (2008) 对长石集合体的变形实验显示在 C'-type 剪切带方位会形成空洞,微观结构也表明变形由颗粒边界扩散控制的蠕变完成,在 GBS 过程中,孔隙的生长和聚结形成空洞 (可能起源于三联点和晶界),它们也是残余孔隙流体的储存槽,说明下地壳可能具有一定的渗透性。长石在相同变

形条件下的异同见图 15。

2.4 长石滑移系

长石有多组滑移系。对于三斜晶系的斜长石而言,低对称性使它的旋转轴和角度具唯一性 (Prior et al., 2009)。当位错攀移形成低角度边界 (< 10°) 时,晶格取向差轴与滑移面有特定的几何关系,滑移方向取决于低角度亚颗粒边界的形成方式是刃型位错还是螺旋位错 (Kruse et al., 2001; Reddy et al., 2007),取向差轴垂直于特定滑移系的面是螺旋位错作用在这个滑移系,而取向差轴在一个滑移面里是刃型位错作用在该滑移系 (Kruse et al., 2001)。Kruse et al. (2001) 总结了斜长石的已知滑移系 (图 16)。斜长石的 (010) 面被认为是最易滑移的面,随后是 (110),最后是 (111) (Gandais et al., 1984), [100] 滑移方向在天然变形斜长石中普遍存在 (Mehl et al., 2008; Hansen et al., 2013)。CPO 数据显示 {111} <110> 和

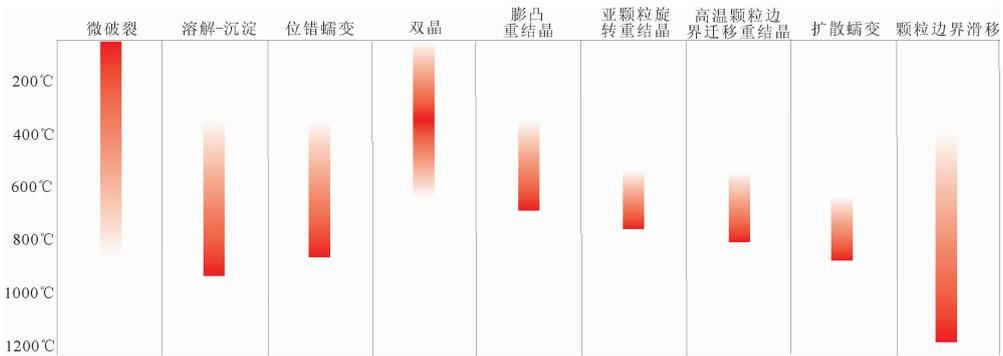


图 15 长石随着温度升高和压力增大的显微变形机制的变化,详见文中描述

Fig. 15 Transition of micro-deformation mechanism of feldspars with increasing temperature and pressure, see the description in the text

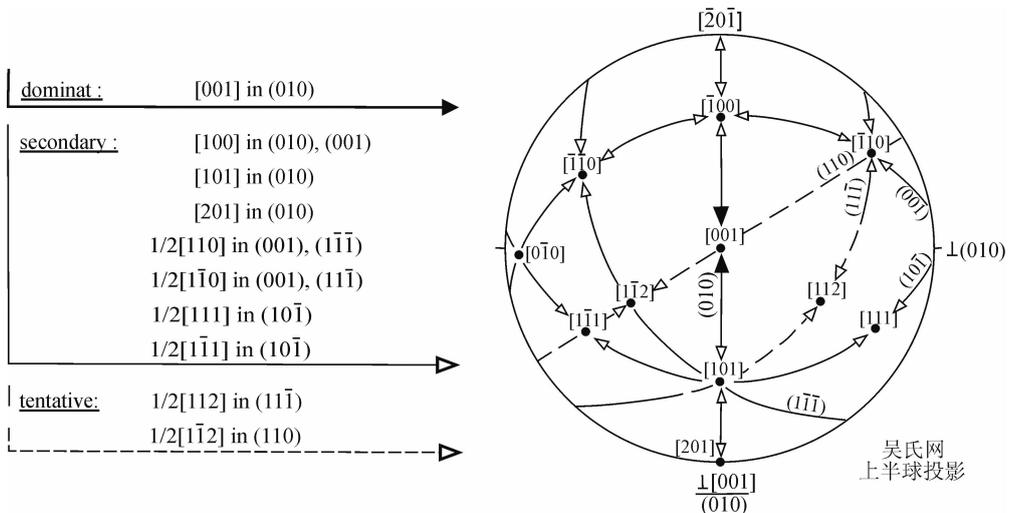


图 16 斜长石的已知滑移系 (C-1 space group) 立体投影图 (Kruse et al., 2001)

Fig. 16 The stereographic projection of the known slip systems of plagioclase (C-1 space group) (Kruse et al., 2001)

(011) $[-100]$ 可能是斜长石的主要滑移系 (Hansen et al. 2013; Andrew, 2015; Miranda et al., 2016)。在 675~700°C 和较高应变环境, 斜长石碎斑中 (010) $\langle 001 \rangle$ 和 (021) $\langle 1-12 \rangle$ 是 (001) $\langle 110 \rangle$ 的辅助滑移系 (Svahnberg et al., 2010)。对实验变形的斜长石而言, 因为位错的有限攀移, 迁移主导的重结晶变形作用最重要 (Tullis et al., 1987, 1990), 重结晶作用受微破裂的影响也较大 (Tullis et al., 1992; McLaren et al., 2001)。Menegon et al. (2008) 总结了钾长石的常见滑移系 (表 1)。

表 1 钾长石的常见滑移系 (Menegon et al., 2008)

Table 1 Active slip system of K-feldspar (Menegon et al., 2008)

参考文献	条件	滑移面	滑移方向	观察方法
实验变形:				
Tullis and Yund (1977)	900-1000°C, 10-15 kb, 10^{-6} /s	(010)	未确定	透射电子显微镜
Willaime et al., (1979) and Scandale et al., (1983)	700°C, 15 kb, 10^{-6} /s	(010) (001) (1-2-1) (010) (110) (1-1-1)	[101] $\frac{1}{2}[110]$ [101] [001] $\frac{1}{2}[1-12]$ $\frac{1}{2}[110]$	透射电子显微镜
	900°C, 15 kb, 10^{-6} /s	(010) (001) (1-2-1) (010)	[101] $\frac{1}{2}[110]$ [101] [110]	
天然变形:				
Debat et al., (1978)	500°C, 2 kb	(010) (110)	未确定 未确定	光学显微镜
Sacerdoti et al., (1980)	500°C, 2 kb	(12-1) (010) (010) (010) (010)	[101] [101] [100] [010] $\frac{1}{2}[1-12]$	透射电子显微镜
Schulmann et al., (1996)	550-600°C, 4-8 kb	(010) (010)	[001] [100]	费氏台
Martelat et al., (1999)	700-800°C, 4-10 kb	(010) (001)	[100] [100]	费氏台
Franek et al., (2006)	700-800°C, 5-8 kb	(010)	[001]	电子背散射衍射
Ishii et al., (2007)	高绿片岩相	(100) (101)	[010] [010]	电子背散射衍射

2.5 不同显微变形机制对长石 CPO 的影响

变形岩石中长石的 CPO 表现受控于长石所经历的变形机制。如果微破裂是沿晶体解理面发育的, 这种变形机制下长石会形成较强的 CPO (Tullis et al., 1992; Imon et al., 2004)。实验岩石学和数值模拟的研究表明长石颗粒的 CPO 可能由溶解-沉淀蠕变形成 (Heidelbach et al., 2000), 在低剪切应变 ($\gamma \leq 3$) 的变形集合体中, 溶解-沉淀蠕变联合矿物颗粒的刚体旋转会形成 CPO, 它的演化可能受控于溶解和生长速率、化学势梯度和晶内流体中溶解物质的扩散速率等 (Bons et al., 2000)。对天然变形长石的研究表明, 溶解-沉淀变形过程形成的 CPO 也受控于相邻母颗粒的晶体特性 (Menegon et al., 2008; Brander et al., 2012; Fukuda et al., 2012)。在高碎斑/沉淀颗粒比率的

岩石中, 新生钾长石颗粒的外延生长会阻碍 CPO 的发育, 新颗粒倾向于随机排列, 但在低碎斑/沉淀颗粒比率的岩石中, 溶解-沉淀蠕变占主导, 形成弱 CPO, 这可能与钾长石的结晶控制反应速率 (或溶解/生长速率) 的低各向异性有关 (Menegon et al., 2008)。因此, 沿变形长石解理面发育的微破裂会造成较强的 CPO; 而受溶解-沉淀作用影响形成的 CPO 较弱, 但它的影响较复杂, 取决于矿物颗粒溶解/生长的各向异性、相邻颗粒的晶体特征等。

在位错蠕变期间, 位错在特定晶格面上移动, 主要由最简单滑移系上的滑动来调节, 在变形过程中, 颗粒会朝促进主滑移系滑动的方向旋转, 形成明显的 CPO (Berger et al., 1996; Passchier et al., 2005), 相比之下, 经历 GBS 的岩石会形成较弱的 CPO (Svahnberg et al., 2010; Viegas et al., 2016)。例如, 弱和随机的 CPO, 及已存在 CPO 的弱化被认为是扩散调节的 GBS 主导的变形造成的 (Bestmann et al., 2003; Warren et al., 2006)。在相对较低的温度条件下, 变形系统中有水但无部分熔融时, 流体能有效增强长石中扩散和位错蠕变调节的 GBS (Tullis et al., 1991), 以至于在岩石变形过程中 CPO 被弱化。此外, 作为 DisGBS 的标志, 重结晶颗粒间的晶体取向差轴可能受控于变形运动学, 而与晶体学特征无关 (Prior et al., 2007), 而且弱-中等 CPO 的发展应该在最简单的滑动系上发生 (Warren et al., 2006), 并且该滑移系应该与相邻碎斑内亚颗粒边界上推导出的滑移系不同 (Prior et al., 2007)。因此, DisGBS 可能造成变形长石形成弱-中的 CPO (Svahnberg et al., 2010; Hansen et al., 2011)。

在扩散蠕变伴随刚体旋转的过程中, 长石中的各向异性扩散率和定向生长很常见 (Tullis et al., 1996), 而这也被认为可以形成一定强度的 CPO (Heidelbach et al., 2000; Fukuda et al., 2012; Negrini et al., 2014)。天然变形的长石基质中形成的弱 CPO 归因于扩散蠕变过程中的各向异性生长 (Menegon et al., 2013), 数值模拟的结果也显示在扩散蠕变过程中各向异性溶解和生长速率可以产生一定强度的 CPO, 其中更快溶解/生长速率的结晶方向最终与粘性流动期间的瞬时拉伸轴一致 (Bons et al., 2000)。斜长石中不同类质同象的相混合与扩散蠕变相结合有助于增强 GBS 而非位错蠕变, 此时, 粒径较小的重结晶颗粒和弱 (或随机) 的 CPO 共同出现被认为是扩散蠕变的微观证据

(Mehl et al., 2008; Raimbourg et al., 2008; Pearce et al., 2011), 理论研究表明, 在扩散蠕变过程中需要 GBS (Raj et al., 1971), 由于晶粒粒径、相比和沿颗粒边界的曲率的变化, GBS 和关联颗粒会造成颗粒旋转, 从而使扩散蠕变期间先存的 CPO 随机化 (Mehl et al., 2008)。因此, 受位错蠕变影响的变形长石会形成明显的 CPO, 而经历 GBS 或扩散蠕变的变形长石, CPO 会被弱化或者彻底消除。

3 显微变形研究方法和技术的最新进展

自然界中长英质糜棱岩是研究应变集中的主要对象, 也是前人研究岩石变形行为的主要物质 (Pennacchioni et al., 2010; Oliot et al., 2010; Kilian et al., 2011; Sullivan et al., 2013; Czaplinska et al., 2015)。例如, 在长石变形中位错蠕变加速 GBS 从而加剧应变集中的研究就是基于角闪辉长糜棱岩中的变形斜长石开展的 (Svahnberg et al., 2010; Miranda et al., 2016)。不同学者研究造山带内天然变形岩石后提出应变局部化容易在熔体弱化带发生 (Slagstad, 2005; Schulmann et al., 2008; Lexa et al., 2011)。由此可见, 多数变形机制和变形过程都是在研究自然界变形岩石的过程中发现的, 对于自然界已发生变形岩石的研究将会是一个永恒的课题。

利用 TEM (透射电子显微镜), 有学者详细观测并确认了长石的滑移系 (Sacerdoti et al., 1980; Scandale et al., 1983)。SEM (扫描电子显微镜) 在显微构造中的应用也很广泛, 例如 Vos et al. (2014) 利用 SEM 系统分析了石英颗粒表明的显微结构, 以此判断其沉积环境和历史。近年来 EBSD (电子背散射衍射) 技术在地质学中的应用也越发成熟, 有学者介绍了 EBSD 技术在大陆动力学研究和地壳构造变形中的应用 (Xu Zhiqin et al., 2009; Huang Xuemeng et al., 2016), 而高清 EBSD 技术的发展也使得地质学们对自然界变形岩石的研究越发深入 (Enami et al., 2017; Wallis et al., 2017)。此外, 近年来显微构造结合岩石磁性组构的研究也越来越被广泛的应用 (Borradaile et al., 2004; Silva et al., 2014; Ghosh et al., 2018; Das et al., 2019)。

地壳地幔流变学模型的建立离不开实验岩石学的贡献, 多数地壳地幔变形参数的估算来自实验数

据的外推 (Tullis, 2002; Okudaira et al., 2012)。实验岩石学可以精确控制物质成分、变形温度、压力、差应力、应变量和应变速率等参数, 因此有其优越的一面。该方法曾被用来研究长石 GBS 过程中伴随的其它应变机制 (Mukherjee et al., 1996; Wakai et al., 1999; Negrini et al., 2014)。此外, 部分熔融岩石中熔体的迁移与聚集对差应力的响应, 也是通过应用实验岩石学来开展研究的 (Zimmerman et al., 2004; Kohlstedt et al., 2009; King et al., 2009)。由于实验岩石学能控制变形过程, 记录变形过程中物理、化学的详细变化, 因此它是研究岩石变形过程中必不可少的方法。

随着计算机技术的发展, 数值模拟逐渐应用到显微变形机制的研究中, 早期主要应用在线性粘性基质中强硬椭球体的变形行为 (Ghosh et al., 1976), 以及塑性晶体的各向异性如何改变冰的动态重结晶作用 (Kamb, 1972) 等研究中。显微构造数值模拟最常用的软件是 Elle (模拟变形和变质过程中显微结构演化的开源软件), 它可以与不同程序相结合来模拟不同的变形变质条件, 例如 Elle 结合基于特定算法的 VPFIT 软件 (该软件采用快速傅里叶变换插值法), 可以对具各向异性的多晶集合体进行塑性变形模拟; 或与 Basil 结合计算不同边界条件下的粘性应变速率及应力场特征 (Ran et al., 2018)。Elle 也曾被应用在研究应变集中、熔融过程等 (Jessell et al., 2005; Becker et al., 2008)。随着显微构造数值模拟的发展, 使我们拥有了检验边界条件、物质属性和观察显微结构动态发展的能力, 提升了我们对自然界和实验中观察到的显微构造现象的认识, 更为重要的是, 结合多个变形机制或考虑先存各向异性的模拟模型, 大大改善了地质学家思考显微动力学系统的研究方法 (Jessell et al., 2005; Gardner et al., 2017; Piazzolo et al., 2018)。此外, 通过提取模拟结果中指示特定显微结构的参数, 可以更好的解释自然界中的显微构造现象 (Piazzolo et al., 2002; Gomez-Rivas et al., 2017; Llorens et al., 2017; Steinbach et al., 2017)。当然显微变形模拟也有未解决的难题, 例如扩散蠕变相关模型并未被加入到模拟当中, 需要进一步发展该研究方法 (Ford et al., 2004)。但是, 最新的数值模拟方法加入了化学过程, 可以把化学过程和应力应变很好的耦合起来, 这成为了当前最为前沿的显微构造模拟方向 (Zhong et al., 2017)。

4 结论

基于前文内容,通过总结不同显微变形机制在长石矿物中的规律,得出以下几个结论:

(1)在上地壳至下地壳环境,长石均出现破裂作用,随着温度增高,破裂作用减弱。在中下地壳环境,长石遭受各种变形机制的耦合,溶解—沉淀作用、位错蠕变和 GBS 尤其活跃。在超高温环境下,GBS 是长石的主导变形机制;

(2)在中低级变质条件下,斜长石和钾长石具类似的显微变形机制,但在高级变质条件下,两者呈现不同的显微变形机制,斜长石更易发生动态重结晶作用,而钾长石更具脆性;

(3)长石变形过程中形成的 CPO 受多种显微变形机制的影响。沿解理面发育的微破裂和位错蠕变变形会使变形长石形成较强的 CPO,而受 GBS 或扩散蠕变影响时,变形长石的 CPO 会被弱化。需要注意的是,长石变形过程中多种变形机制会耦合或迭代,CPO 也会随之改变,所以不能单纯的利用 CPO 的形态来判断岩石所经历的显微变形机制。

相比石英,地质学家们对长石变形机制的研究程度较低,而长石是中下地壳最主要的造岩矿物,它的变形行为更能影响中下地壳的流变学属性。条纹长石是由钾长石和钠斜长石共同组成的特殊长石,是研究固溶相流变学的良好载体,相比斜长石和钾长石,对条纹长石的研究程度更低,它的显微变形特征可能更贴近长石的变形属性。所以对条纹长石的研究可能进一步扩展我们对长石变形特征的理解,进而为解锁中下地壳流变学属性提供新思路。

致谢:感谢李海兵研究员在成文过程中给予的鼓励,也感谢审稿专家提出的建设性意见与建议,对提高论文质量有很大的帮助。

References

Altenberger U, Wilhelm S. 2000. Ductile deformation of K-feldspar in dry eclogite facies shear zones in the Bergen Arcs, Norway. *Tectonophysics*, 320(2): 107~121.

Álvarez-Valero A M, Cesare B, Kriegsman L M. 2005. Formation of elliptical garnet in a metapelitic enclave by melt-assisted dissolution and reprecipitation. *Journal of Metamorphic Geology*, 23(2): 65~74.

Andrew J C. 2015. Microstructural evolution under non-steady state deformation in mid-crustal ductile shear zones. University of Otago (PHD thesis).

Austin N, Evans B. 2009. The kinetics of microstructural evolution during deformation of calcite. *Journal of Geophysical Research: Solid Earth*, 114(B9).

Beaumont C, Nguyen M H, Jamieson R A, Ellis S. 2006. Crustal flow modes in large hot orogens. *Geological Society London*

Special Publications, 268(1): 91~145.

Becker J K, Bons P D, Jessell M W. 2008. A new front-tracking method to model anisotropic grain and phase boundary motion in rocks. *Computers and Geosciences*, 34: 201~212.

Bell T H, Cuff C. 1989. Dissolution, solution transfer, diffusion versus fluid flow and volume loss during deformation/metamorphism. *Journal of Metamorphic Geology*, 7:425~447.

Berger A, Stünitz H. 1996. Deformation mechanisms and reaction of hornblende: examples from the bergell tonalite (central alps). *Tectonophysics*, 257(2~4): 0~174.

Bestmann M, Prior D J. 2003. Intragranular dynamic recrystallization in naturally deformed calcite marble: diffusion accommodated grain boundary sliding as a result of subgrain rotation recrystallization. *Journal of Structural Geology*, 25(10):1597~1613.

Bons P D, Brok B D. 2000. Crystallographic preferred orientation development by dissolution-precipitation creep. *Journal of Structural Geology*, 22(11~12):1713~1722.

Borradaile G J, Jackson M. 2004. Anisotropy of magnetic susceptibility (AMS): magnetic petrofabrics of deformed rocks. *Geological Society London Special Publications*, 238(1): 299~360.

Boullier A M, Guéguen Y. 1998b. Peridotite mylonite produced by superplastic flow. In: Snoko A, Tullis J, Todd V R (eds) *Fault related rocks—a photographic atlas*. New Jersey: Princeton University Press, 592~593.

Brander L, Svahnberg H, Piazzolo S. 2012. Brittle-ductile deformation in initially dry rocks at fluid-present conditions: transient behaviour of feldspar at mid-crustal levels. *Contributions to Mineralogy and Petrology*, 163: 403~425.

Bürgmann R, Dresen G. 2008. Rheology of the lower crust and upper mantle: Evidence from rock mechanics, geodesy, and field observations. *Annual Review of Earth and Planetary Sciences*, 36(1): 531.

Carter N, Kirby S H. 1978. Transient creep and semibrittle behavior of crystalline rocks. *Pure and Applied Geophysics*, 116(4~5): 807~839.

Carter N, Tsenn M. 1987. Flow properties of continental lithosphere. *Tectonophysics*, 136(1~2): 27~63.

Cooper R F, Kohlstedt D L. 1984. Solution-precipitation enhanced diffusional creep of partially molten olivine-basalt aggregates during hot-pressing. *Tectonophysics*, 107(3~4): 207~233.

Czaplinska D, Piazzolo S, Zibra I. 2015. The influence of phase and grain size distribution on the dynamics of strain localization in polymineralic rocks. *Journal of Structural Geology*, 72: 15~32.

Das P, Mukherjee S, Das K, Ghosh G. 2019. Integrating AMS data with structural studies from granitoid rocks of the eastern Dharwar Craton, south India: Implications on successive fabric development and regional tectonics. *Journal of Structural Geology*, 118: 48~67.

De Ronde A, Stünitz H, Tullis J, Heilbronner R. 2005. Reaction-induced weakening of plagioclase-olivine composites. *Tectonophysics*, 409: 85~106.

Debat P, Soula J C, Kubin L, Vidal J L. 1978. Optical studies of natural deformation microstructures in feldspars (gneiss and pegmatites from Occitania, southern France). *Lithos*, 11:133~145.

Dell' Angelo L N, Tullis J. 1988. Experimental deformation of partially melted granitic aggregates. *Journal of Metamorphic Geology*, 6(4):21.

Dimanov A, Rybacki E, Wirth R, Dresen G. 2007. Creep and strain-dependent microstructures of synthetic anorthite-diopside aggregates. *Journal of Structural Geology*, 29(6): 1049~1069.

Egydio-Silva M, Mainprice D. 1999. Determination of stress directions from plagioclase fabrics in high grade deformed rocks (Além Paraíba shear zone, Ribeira fold belt, southeastern Brazil). *Journal of Structural Geology*, 21(12):1751~1771.

Ellis S, Stöckhert B. 2004. Imposed strain localization in the lower

- crust on seismic timescales. *Earth, Planets, and Space*, 56 (12):1103~1109.
- Ellsworth W, Hickman S, Zoback M, Davis E, Gee L, Huggins R et al. 2005. Observing the san andreas fault at depth. In: AGU Fall Meeting Abstracts, 1: 04.
- Enami M, Nagaya T, Win M M. 2017. An integrated EPMA~EBSD study of metamorphic histories recorded in garnet. *American Mineralogist*, 102(1): 192~204.
- Evans B, Renner J, Hirth G. 2001. A few remarks on the kinetics of static grain growth in rocks. *International Journal of Earth Science*, 90(1): 88~103.
- Fliervoet T F, White S H, Drury M R. 1997. Evidence for dominant grain boundary sliding in greenschist and amphibolite facies conditions from the redbank deformed zone, central australia. *Journal of Structural Geology*, 19(12):1495~1520.
- Ford J M, Wheeler J. 2004. Modelling interface diffusion creep in two-phase materials. *Acta Mater*, 52: 2365~2376.
- Franek J, Schulmann K, Lexa O. 2006. Kinematic and rheological model of exhumation of high pressure granulites in the Variscan orogenic root; Example of the Blansky les granulite, Bohemian Massif, Czech Republic. *Mineralogy and Petrology*, 86: 253~276.
- Franek J, Schulmann K, Lexa O, Ulrich S, Stipska P, Haloda J, Tycova P. 2011. Origin of felsic granulite microstructure by heterogeneous decomposition of alkali feldspar and extreme weakening of orogenic lower crust during the variscan orogeny. *Journal of Metamorphic Geology* 29: 103~130.
- Fukuda J, Okudaira T. 2013. Grain-size-sensitive creep of plagioclase accompanied by solution-precipitation and mass transfer under mid-crustal conditions. *Journal of Structural Geology*, 51:61~73.
- Fukuda J, Okudaira T, Satsukawa T, Michibayashi K. 2012. Solution-precipitation of K-feldspar in deformed granulites and its relationship to the distribution of water. *Tectonophysics*, 532~535: 175~185.
- Gandais M, Willaime C. 1984. Mechanical Properties of Feldspars. *Feldspars and Feldspathoids*, 137: 207~246.
- Gardner R, Piazzolo S, Evans L, Daczko N. 2017. Patterns of strain localization in heterogeneous, polycrystalline rocks—a numerical perspective. *Earth and Planetary Science Letters*, 463: 253~265.
- Ghosh B, Das P, Sarkar D P, Ghosh G, Mukhopadhyay J, Ando J I. 2018. Coalescing microstructure and fabric transitions with AMS data in deformed lime-stone; Implications on deformation kinematics. *Journal of Structural Geology*, 114:249~309.
- Ghosh S K, Ramberg H. 1976. Reorientation of inclusions by combination of pure shear and simple shear. *Tectonophysics*, 34 (1~2):1~70.
- Goetze C, Evans B. 1979. Stress and temperature in the bending lithosphere as constrained by experimental rock mechanics. *Geophysical Journal of the Royal Astronomical Society*, 59(3): 463~478.
- Gomez~Rivas E, Griera A, Llorens M G, Bons P D, Lebensohn R A and Piazzolo S 2017. Subgrain rotation recrystallization during shearing: Insights from full-field numerical simulations of halite polycrystals. *Journal of Geophysical Research: Solid Earth*, 122 (11): 8810~8827.
- Gower R J W, Simpson C. 1992. Phase boundary mobility in naturally deformed, high-grade quartzofeldspathic rocks; Evidence for diffusional creep. *Journal of Structural Geology*, 14 (3):301~313.
- Gratier J P, François R, Labaume P. 1999. How pressure solution creep and fracturing processes interact in the upper crust to make it behave in both a brittle and viscous manner. *Journal of Structural Geology*, 21(8-9): 1189~1197.
- Guillope M, Poirier J P. 1979. Dynamic recrystallization during creep of single-crystalline halite; An experimental study. *Journal of Geophysical Research Solid Earth*, 84 (B10): 5557~5567.
- Hansen L N, Cheadle M J, John B E, Swapp S M, Dick H J B, Tucholke B E, Tivey M A. 2013. Mylonitic deformation at the Kane oceanic core complex; Implications for the rheological behavior of oceanic detachment faults. *Geochemistry, Geophysics, Geosystems*, 14: 3085~3108.
- Hansen L N, Zimmerman M E, Kohlstedt D L. 2011. Grain boundary sliding in San Carlos olivine; Flow law parameters and crystallographic-preferred orientation. *Journal of Geophysical Research: Solid Earth*, 116:1~16.
- Heidelbach F, Post A, Tullis J. 2000. Crystallographic preferred orientation in albite samples deformed experimentally by dislocation and solution precipitation creep. *Journal of Structural Geology*, 22:1649~1661.
- Herwegh M, Linckens J, Ebert A, Berger A, Brodhag S H. 2011. The role of second phases for controlling microstructural evolution in polymineralic rocks; A review. *Journal of Structural Geology*, 33(12):1728~1750.
- Heyes G W, Allan G C, Bruckard W J, Sparrow G J. 2012. Review of flotation of feldspar. *Transactions of the institution of Mining and Metallurgy*, 121(2): 72~78.
- Hippert J F M. 1994. Grain boundary microstructures in micaceous quartzite; Significance for fluid movement and deformation processes in low metamorphic grade shear zones. *Geology*, 102: 331~348.
- Hirth G, Kohlstedt D. 1995. Experimental constraints on the dynamics of the partially molten upper mantle; Deformation in the diffusion creep regime. *Journal of Geophysical Research: Solid Earth*, 100(B2):1981~2001.
- Hirth G, Kohlstedt D. 2003. Rheology of the upper mantle and the mantle wedge; A view from the experimentalists. *Geophysical Monograph Series*, 138: 83~105.
- Hirth G, Tullis J. 1992. Dislocation creep regimes in quartz aggregates. *Journal of Structural Geology*, 14(2):145~159.
- Huang Xuemeng, Zhang Jinjiang, Xu Zhiqin. 2016. The Application of EBSD in the Study of Crustal Structural Deformation. *Acta Geologica Sinica*, 90(6): 1130~1145 (in Chinese with English abstract).
- Hunter N J R, Weinberg R F, Wilson C J L, Luzin V, Misra S. 2018. Quartz deformation across interlayered monomineralic and polymineralic rocks; A comparative analysis. *Journal of Structural Geology*, 119 (2019): 118~134.
- Imon R, Okudaira T, Kanagawa K. 2004. Development of shape and lattice preferred orientations of amphibole grains during initial cataclastic deformation and subsequent deformation by dissolution-precipitation creep in amphibolites from the Ryoke metamorphic belt, SW Japan. *Journal of Structural Geology*, 26 (5):793~805.
- Ingebritsen S E, Manning C E. 2010. Permeability of the continental crust; dynamic variations inferred from seismicity and metamorphism. *Geofluids*, 10 (1~2):193~205.
- Ishii K, Kanagawa K, Shigematsu N, Okudaira T. 2007. High ductility of K-feldspar and development of granitic banded ultramylonite in the Ryoke metamorphic belt, SW Japan. *Journal of Structural Geology* 29: 1083~1098.
- Jessell M W, Kostenko O, Jamtveit B. 2003. The preservation potential of microstructures during static grain growth. *Journal of Metamorphic Geology*, 21(5): 11.
- Jessell M W, Siebert E, Bons P D, Evans L, Piazzolo S. 2005. A new type of numerical experiment on the spatial and temporal patterns of localization of deformation in a material with a coupling of grain size and rheology. *Earth and Planetary Science Letters*, 239: 309~326.
- Ji S, Mainprice D. 1990. Recrystallization and Fabric Development in Plagioclase. *The Journal of Geology*, 98(1): 65~79.
- Jiang Z, Prior D J, Wheeler J. 2000. Albite crystallographic preferred orientation and grain misorientation distribution in a low-grade mylonite; Implications for granular flow. *Journal of Structural Geology*, 22: 1663~1674.
- Kamb W B. 1972. Experimental recrystallization of ice under stress.

- American Geophysical Union Monograph, 16: 221~241.
- Kanagawa K, Shimano H, Hiroi Y. 2008. Mylonitic deformation of gabbro in the lower crust; a case study from the Pankenushi gabbro in the Hidaka metamorphic belt of central Hokkaido, Japan. *Journal of Structural Geology*, 30:1150~1166.
- Kassner M E, Hayes T A. 2003. Creep cavitation in metals. *International Journal of Plasticity*, 19(10): 1715~1748.
- Kenis I, Urai J L, van der Zee, Hilgers W, Sintubin C M. 2005. Rheology of fine-grained siliciclastic rocks in the middle crust-evidence from structural and numerical analysis. *Earth and Planetary Science Letters*, 233: 351~360.
- Kenkmann T, Dresen G. 2002. Dislocation microstructure and phase distribution in a lower crustal shear zone: An example from the Ivrea-Zone, Italy. *International Journal of Earth Sciences*, 91(3):445~458.
- Kenkmann T. 2000. Processes controlling the shrinkage of porphyroclasts in gabbroic shear zones. *Journal of Structural Geology*, 22(4):471~487.
- Kilian R, Heilbronner R, Stünitz H. 2011. Quartz grain size reduction in a granitoid rock and the transition from dislocation to diffusion creep. *Journal of Structural Geology*, 33: 1265~1284.
- King D S H, Zimmerman M E, Kohlstedt D L. 2009. Stress-driven melt segregation in partially molten olivine-rich rocks deformed in torsion. *Journal of Petrology*, 51(1~2): 21~42.
- Kirby S H, Stern L A. 1993. Experimental dynamic metamorphism of mineral single crystals. *Journal of Structural Geology*, 15 (9~10):1223~1240.
- Kirby S H. 1983. Rheology of the lithosphere. *Reviews of Geophysics*, 21(6):1458~1487.
- Knipe R J. 1989. Deformation mechanisms; recognition from natural tectonites. *Journal of Structural Geology*, 11(1):127~146.
- Kohlstedt D L, Holtzman B K. 2009. Shearing melt out of the Earth: An experimentalist's perspective on the influence of deformation on melt extraction. *Annual Review of Earth and Planetary Sciences*, 37 (1): 561~593.
- Krabbendam M, Urai J L, Van Vliet L J. 2003. Grain size stabilisation by dispersed graphite in a high-grade quartz mylonite; an example from Naxos (Greece). *Journal of Structural Geology*, 25(6): 855~866.
- Kruhl J H. 2001. Crystallographic control on the development of foam textures in quartz, plagioclase and analogue material. *International Journal of Earth Sciences*, 90(1):104~117.
- Kruse R, Stünitz H, Kunze K. 2001. Dynamic recrystallization processes in plagioclase porphyroclasts. *Journal of Structural Geology*, 23 (11):1781~1802.
- Küster M, Stöckhert B. 1999. High differential stress and sublithostatic pore fluid pressure in the ductile regime-microstructural evidence for short-term post-seismic creep in the Sesia Zone, Western Alps. *Tectonophysics*, 303 (1): 263~277.
- Lafrance B, John B E, Scoates J S. 1996. Syn-emplacement recrystallization and deformation microstructures in the Poe Mountain anorthosite, Wyoming. *Contributions to Mineralogy and Petrology*, 122(4): 431~440.
- Lehner F K. 1995. A model of intergranular pressure solution in open systems. *Tectonophysics*, 245:153~170.
- Lexa O, Schulmann K, Janoušek V, Štípská P, Guy A, Racek M. 2011. Heat sources and trigger mechanisms of exhumation of HP granulites in Variscan orogenic root. *Journal of Metamorphic Geology*, 29(1): 79~102.
- Li Hailong, Song Chuansong, Han Jianjun, Li Jiahao, Ren Shenglian, Zhang Yan, Wang Wei, Yang Fan, Li Zhenwei, Wang Yangyang, Yuan Fang, Lan Ruixuan. 2017. Study on the Structural Deformation Characteristics of the Shear Zone in the Northern Boundary of the Tongbai Complex. *Geological Review*, 63(3):677~693 (in Chinese with English abstract).
- Llorens M G, Griera A, Steinbach F, Bons P D, Gomez~Rivas E, Jansen D, Roessiger J, Lebensohn R A, Weikusat I. 2017. Dynamic recrystallization during deformation of polycrystalline ice: insights from numerical simulations. *Philosophical Transactions of the Royal Society London, Series A (Mathematical, Physical and Engineering Sciences)*, 375 (2086): 1364~503X.
- Lloyd G E, Freeman B. 1994. Dynamic recrystallization of quartz under greenschist conditions. *Journal of Structural Geology*, 16 (6):867~881.
- Lund M D, Piaolo S, Harley S L. 2006. Ultrahigh temperature deformation microstructures in felsic granulites of the Napier Complex, Antarctica. *Tectonophysics*, 427(1~4):0~151.
- Mancktelow N S, Pennacchioni G. 2004. The influence of grain boundary fluids on the microstructure of quartz-feldspar mylonites. *Journal of Structural Geology*, 26(1):47~69.
- Mancktelow N S, Pennacchioni G. 2005. The control of precursor brittle fracture and fluid-rock interaction on the development of single and paired ductile shear zones. *Journal of Structural Geology*, 27(4):645~661.
- Martelat J E, Schulmann K, Lardeaux J M, Nicollet C, Cardon H. 2006. Granulite microfabrics and deformation mechanisms in southern Madagascar. *Journal of Structural Geology* 21(6): 671~687.
- Mclaren A C, Pryer L. 2001. Microstructural investigation of the interaction and interdependence of cataclastic and plastic mechanisms in Feldspar crystals deformed in the semi-brittle field. *Tectonophysics*, 335(1):1~15.
- Mehl L, Hirth G. 2008. Plagioclase preferred orientation in layered mylonites; Evaluation of flow laws for the lower crust. *Journal of Geophysical Research: Solid Earth*, 113(B5):0148~0227.
- Menegon L, Pennacchioni G, Spiess R. 2008. Dissolution-precipitation creep of K-feldspar in mid-crustal granite mylonites. *Journal of Structural Geology*, 30 (5):565~579.
- Menegon L, Pennacchioni G, Stünitz H. 2006. Nucleation and growth of myrmekite during ductile shear deformation in metagranites. *Journal of Metamorphic Geology*, 24(7):17.
- Menegon L, Stünitz H, Nasipuri P, Heilbronner R, Svahnberg H. 2013. Transition from fracturing to viscous flow in granulite facies perthitic feldspar (Lofoten, Norway). *Journal of Structural Geology*, 48: 95~111.
- Miranda E A, Hirth G, John B E. 2016. Microstructural evidence for the transition from dislocation creep to dislocation-accommodated grain boundary sliding in naturally deformed plagioclase. *Journal of Structural Geology*, 92:30~45.
- Montési L G J, Hirth G. 2003. Grain size evolution and the rheology of ductile shear zones; From laboratory experiments to postseismic creep. *Earth and Planetary Science Letters*, 211: 97~110.
- Mukherjee A K, Zelin M G. 1996. Geometrical aspects of superplastic flow. *Materials Science and Engineering*, 208(2): 210~225.
- Negrini M, Stünitz H, Nasipuri P, Menegon L, Morales L F G. 2014. Semibrittle deformation and partial melting of perthitic K-feldspar; An experimental study. *Journal of Geophysical Research: Solid Earth*, 119:3478~3502.
- Nishikawa O, Takeshita T. 2000. Progressive lattice misorientation and microstructural development in quartz veins deformed under subgreenschist conditions. *Journal of Structural Geology*, 22 (2):259~276.
- Okudaira T, Shigematsu N. 2012. Estimates of stress and strain rate in mylonites based on the boundary between the fields of grain-size sensitive and insensitive creep. *Journal of Geophysical Research*, 117:3210~3224.
- Oliot E, Goncalves P, Marquer D. 2010. Role of plagioclase and reaction softening in a metagranite shear zone at mid-crustal conditions (Gotthard Massif, Swiss Central Alps). *Journal of Metamorphic Geology*, 28(8): 849~871.
- Passchier C W, Trouw R A J. 2005. *Microtectonics*. Germany: Springer, 26~66.

- Paterson M S. 1995. A theory for granular flow accommodated by material transfer via intergranular fluid. *Tectonophysics*, 245(3~4):135~151.
- Pearce M A, Wheeler J, Prior D J. 2011. Relative strength of mafic and felsic rocks during amphibolite facies metamorphism and deformation. *Journal of Structural Geology* 33, 662~675.
- Pennacchioni G, Menegon L, Leiss B, Nestola F, Bromiley G. 2010. Development of crystallographic preferred orientation and microstructure during plastic deformation of natural coarse grained quartz veins. *Journal of Geophysical Research: Solid Earth*, 115(12):148~227.
- Piazolo S, Bons P D, Griera A, Llorens M G, Gomez~Rivas E, Koehn D, Wheeler J, Gardner R, Godinho J R A, Evans L, Lebensohn R A, Jessell M W. 2018. A review of numerical modelling of the dynamics of microstructural development in rocks and ice: Past, present and future. *Journal of Structural Geology*, in press Piazolo S, Bons P D, Jessell M W, Evans L, Passchier C W. 2002. Dominance of microstructural processes and their effect on microstructural development: insights from numerical modelling of dynamic recrystallization. *Geological Society, London, Special Publications*, 200(1):149~170.
- Prior D J, Hirth G. 2007. Microstructural recognition of grain boundary sliding and its rheological implications. *Rendiconti della SocietaGeologica Italiana*, 5:187.
- Pryer L L, Robin P Y F. 1996. Differential stress control on the growth and orientation of flame perthite: A palaeostress-direction indicator. *Journal of Structural Geology*, 18(9):1151~1166.
- Pryer L L. 1993. Microstructures in feldspars from a major crustal thrust zone: The Grenville Front, Ontario, Canada. *Journal of structural Geology*, 15(1):21~36.
- QinXuping, Li Dewei, Xu Hansheng, Liu Jianxiang, Mao Chen, Xu Yexi. 2018. Yanshanian thermo-upwelling extension and palaeo-hydrothermal system in southeast Guangdong: A case study of Enping-Xinfeng detachment fault. *Geology in China*, 45(6): 1188~1204 (in Chinese with English abstract).
- Raimbourg H, Toyoshima T, Harima Y, Kimura G. 2008. Grain-size reduction mechanisms and rheological consequences in high-temperature gabbro mylonites of Hidaka, Japan. *Earth and Planetary Science Letters*, 267(3~4):637~653.
- Raj R, Ashby M F. 1971. On grain boundary sliding and diffusional creep. *Metallurgical and Materials Transactions*, 2(4):1113~1127.
- Ramsay J. 1980. Shear zone geometry: A review. *Journal of Structural Geology*, 2(1):83~99.
- Ran H, DeRiese T, Llorens M G, Finch M A, Evans L, Gomez~Rivas E, Griera A, Jessell M W, Lebensohn R A, Piazolo S, Bons P D. 2018. Time for anisotropy: The significance of mechanical anisotropy for the development of deformation structures. *Journal of Structural Geology*, in Press.
- Ree J H, Kim H S, Han R, Jung H. 2005. Grain-size reduction of feldspars by fracturing and neocrystallization in a low-grade granitic mylonite and its rheological effect. *Tectonophysics*, 407: 227~237.
- Regenauer-Lieb K, Yuen D. 2003. Modeling shear zones in geological and planetary sciences: Solid and fluid-thermal-mechanical approaches. *Earth Science Reviews*, 63(3): 295~349.
- Rosenberg C L, Handy M R. 2005. Experimental deformation of partially melted granite revisited: implications for the continental crust. *Journal of Metamorphic Geology*, 23(1):10.
- Rosenberg C L, Stünitz H. 2003. Deformation and recrystallization of plagioclase along a temperature gradient: an example from the Bergell tonalite. *Journal of Structural Geology*, 25(3): 389~408.
- Rutter E H, Casey M, Burlini L. 1994. Preferred crystallographic orientation development during the plastic and superplastic flow of calcite rocks. *Journal of Structural Geology*, 16:1431~1446.
- Rutter E H. 1976. The kinetics of rock deformation by pressure solution. *Philosophical Transactions of the Royal Society London*, A283:203~219.
- Rutter E H. 1995. Experimental study of the influence of stress, temperature, and strain on the dynamic recrystallization of Carrara marble. *Journal of Geophysical Research: Solid Earth*, 100(B12):24651~24663.
- Rybacki E, Dresen G. 2004. Deformation mechanism maps for feldspar rocks. *Tectonophysics*, 382(3~4): 173~187.
- Rybacki E, Wirth R, Dresen G. 2008. High-strain creep of feldspar rocks; Implications for cavitation and ductile failure in the lower crust. *Geophysical Research Letters*, 35(4).
- Sacerdoti M, Labernardiere H, Gandais M. 1980. Transmission electron microscope (TEM) study of geologically deformed potassic feldspars. *Bulletin de Mine'ralogie*, 103:148~155.
- Scandale E, Gandais, M, Willaime C. 1983. Transmission electron microscopic study of experimentally deformed K-feldspar single crystal. The (010) [001], (001) $\frac{1}{2}$ [110], (110) $\frac{1}{2}$ [112] and (111) $\frac{1}{2}$ [110] slip systems. *Physics and Chemistry of Minerals*, 9:182~187.
- Schulmann K, Lexa O, Štípská P, Ráček M, Tajčmanová L, Konopásek J, Edel J B, Peschler A, Lehmann J. 2008. Vertical extrusion and horizontal channel flow of orogenic lower crust: Key exhumation mechanisms in large hot orogens? *Journal of Metamorphic Geology*, 26(2), 273~297.
- Schulmann K, Mlcoch B, Melka R. 1996. High-temperature microstructures and rheology of deformed granite, Erzgebirge, Bohemian Massif. *Journal of Structural Geology*, 18:719~733.
- Shelly, David R. 2010. Migrating tremors illuminate complex deformation beneath the seismogenic San Andreas fault. *Nature*, 463(7281): 648~652.
- Shigematsu N. 1999. Dynamic recrystallization in deformed plagioclase during progressive shear deformation. *Tectonophysics*, 305(4): 437~452.
- Silva P F, Marques F O, Machek M, Henry B, Hirt A M, Roxerová Z, Madureira P, Vratislav S. 2014. Evidence for non-coaxiality of ferromagnetic and paramagneticfabrics, developed during magma flow and cooling in a thick mafic dyke. *Tectonophysics* 629: 155~164.
- Slagstad T. 2005. Formation, crystallization, and migration of melt in the Mid-orogenic crust: Muskok a domain migmatites, Grenville Province, Ontario. *Journal of Petrology*, 46(5): 893~919.
- Steinbach F, Kuiper E J N, Eichler J, Bons P D, Drury M R, Griera A, Pennock G M, Weikusat I. 2017. The relevance of grain dissection for grain size reduction in polar ice: Insights from numerical models and ice core microstructure analysis. *Frontiers in Earth Science*. 5: 66.
- Stel H. 1981. Crystal growth in cataclases; diagnostic microstructures and implications. *Tectonophysics*, 78(1):585~600.
- Stipp M, Stünitz H, Heilbronner R, Schmid S M. 2002. The eastern tonale fault zone: A 'natural laboratory' for crystal plastic deformation of quartz over a temperature range from 250 to 700°C. *Journal of Structural Geology*, 24(12):1861~1884.
- Stünitz H, Fitz Gerald J D. 1993. Deformation of granitoids at low metamorphic grade, II. Granular flow in albite-rich mylonites. *Tectonophysics* 221:299~324.
- Stünitz H, Gerald, J D F, Tullis J. 2003. Dislocation generation, slip systems, and dynamic recrystallization in experimentally deformed plagioclase single crystals. *Tectonophysics*, 372(3): 215~233.
- Stünitz H. 1998. Syndeformational recrystallization: dynamic or compositionally induced? *Contrib Mineral Petrol*, 131: 219~236.
- Sullivan W A, Boyd A S, Monz M E. 2013. Strain localization in homogeneous granite near the brittle-ductile transition; a case study of the Kellyland fault zone, Maine, USA. *Journal of Structural Geology*, 56:70~88.
- Svahnberg H, Piazolo S. 2010. The initiation of strain localisation in plagioclase-rich rocks: Insights from detailed microstructural

- analyses. *Journal of Structural Geology*, 32(10):1404~1416.
- Tapponnier P, Brace W F. 1976. Development of stress-induced microcracks in Westerly Granite. *International Journal of Rock Mechanics and Mining Sciences and Geomechanics Abstracts*, 13(4):103~112.
- Trepmann C A, Stöckhert B. 2003. Quartz microstructures developed during non-steady state plastic flow at rapidly decaying stress and strain rate. *Journal of Structural Geology*, 25(12):2035~2051.
- Trepmann C A, Stöckhert B, Dorner D, Moghadam R H, Küster M, Röller K. 2007. Simulating coseismic deformation of quartz in the middle crust and fabric evolution during postseismic stress relaxation: An experimental study. *Tectonophysics*, 442: 83~104.
- Tullis J, Yund R A. 1977. Experimental deformation of dry Westerly granite. *Journal of Geophysical Research*, 82: 5705~5718.
- Tullis J, Yund R A. 1987. Transition from cataclastic flow to dislocation creep of feldspar: Mechanisms and microstructures. *Geology*, 15(7):606~609.
- Tullis J, Yund R A. 1991. Diffusion creep in feldspar aggregates: experimental evidence. *Journal of Structural Geology*, 13(9): 987~1000.
- Tullis J, Yund R A. 1992. The brittle-ductile transition in feldspar aggregates: An experimental study. In: Evans B, Wong TF (eds) *Fault mechanics and transport properties of rocks: A festschrift in honour of W F Brace*, 89~117.
- Tullis J, Dell'Angelo L, Yund R A. 1990. Ductile shear zones from brittle precursors in feldspathic rocks: The role of dynamic recrystallization. In: Hobbs BE, Heard HC (eds) *Mineral and rock deformation: Laboratory studies*. American Geophysical Union, *Geophys Monogr.* 56:67~81.
- Tullis J, Yund R A, Farver J. 1996. Deformation-enhanced fluid distribution in feldspar aggregates and implications for ductile shear zones. *Geology*, 24(1):63.
- Tullis J. 2002. Deformation of granitic rocks; Experimental studies and natural examples. *Reviews in Mineralogy and Geochemistry*, 51(1):51~95.
- Uenishi K. 2009. Deformation of earth materials; an introduction to the rheology of solid earth by Shun-ichiro Karato. *Pure and Applied Geophysics*, 166(12):2095.
- Vernon R H, Johnson S E, Melis E A. 2004. Emplacement ~ related microstructures in the margin of a deformed pluton: The San José tonalite, Baja California, México. *Journal of Structural Geology*, 26:1867~1884.
- Vernooij M G C, Brok B D, Kunze K. 2006. Development of crystallographic preferred orientations by nucleation and growth of new grains in experimentally deformed quartz single crystals. *Tectonophysics*, 427(1~4):35~53.
- Viegas G, Menegon L, Archanjo C. 2016. Brittle grain-size reduction of feldspar, phase mixing and strain, localization in granitoids at mid-crustal conditions (Pernambuco shear zone, NE Brazil). *Solid Earth*, 7(4):2953~2998.
- Vollbrecht A, Rust S, Weber K. 1991. Development of microcracks in granites during cooling and uplift: Examples from the Variscan basement in NE Bavaria, Germany. *Journal of Structural Geology*, 13(7):787~799.
- Vollbrecht A, Stipp M, Olesen NØ. 1999. Crystallographic orientation of microcracks in quartz and inferred deformation processes: A study on gneisses from the German Continental Deep Drilling Project (KTB). *Tectonophysics*, 303(1~4):279~297.
- Wakai F, Kondo N, Shinoda Y. 1999. Ceramics superplasticity. *Mrs Proceedings*, 601(5):461~465.
- Wallis D, Parsons A J, Hansen L N. 2017. Quantifying geometrically necessary dislocations in quartz using HR~EBSD: Application to chessboard subgrain boundaries. *Journal of Structural Geology*. (in press).
- Walte N P, Bons P D, Passchier C W. 2005. Deformation of melt-bearing systems-insight from in situ grain-scale analogue experiments. *Journal of Structural Geology*, 27(9): 1666~1679.
- Warren J M, Hirth G. 2006. Grain size sensitive deformation mechanisms in naturally deformed peridotites. *Earth and Planetary Science Letters*, 248(1~2):438~450.
- Wheeler J. 1992. Importance of pressure solution and coble creep in the deformation of polymineralic rocks. *Journal of Geophysical Research Solid Earth*, 97(B4):4579~4586.
- White S H, Burrows S E, Carreras J, Shaw N D, Humphreys F J. 1980. On mylonites in ductile shear zones. *Journal of Structural Geology*, 2: 175~187.
- Willaime C, Christie J M, Kovacs M P. 1979. Experimental deformation of K-feldspar single crystals. *Bulletin de Mine'ralogie*, 102:168~177.
- Wintsch R P, Yi K. 2002. Dissolution and replacement creep: A significant deformation mechanism in mid-crustal rocks. *Journal of Structural Geology*, 24(6):1179~1193.
- Xu Longhua, Tian Jia, Wu Houqin, Deng Wei, Yang Yaohui, Sun Wei, Gao Zhiyong, Hu Yuehua. 2017. New insights into the oleate flotation response of feldspar particles of different sizes: Anisotropic adsorption model. *Journal of Colloid and Interface Science*, 505: 500~508.
- Xu Zhiqin, Wang Qin, Liang Fenghua, Chen Fangyuan and Xu Cuiping. 2009. Electron backscatter diffraction (EBSD) technique and its application to study of continental dynamics. *Acta Petrologica Sinica*, 25(7): 1721~1736 (in Chinese with English abstract).
- Zavada P, Schulmann K, Konopasek J, Ulrich S, Lexa O. 2007. Extreme ductility of feldspar aggregates; Melt-enhanced grain boundary sliding and creep failure; Rheological implications for felsic lower crust. *Journal of Geophysical Research: Solid Earth*, 112(B10):148~227.
- Zhang Ye, Hu Yuehua, Sun Ning, Liu Runqing, Wang Zhen, Wang Li, Sun Wei. 2018. Systematic review of feldspar beneficiation and its comprehensive application. *Minerals Engineering*, 128: 141~152.
- Zhong X, Vrijmoed J, Moulas E, Tajčmanová L. 2017. A coupled model for intragranular deformation and chemical diffusion. *Earth and Planetary Science Letters*, 474: 387~396.
- Zimmerman M E, Kohlstedt D L. 2004. Rheological properties of partially molten lherzolite. *Journal of Structural Geology*, 45: 275~298.

参 考 文 献

- 常丽华, 陈曼云, 金巍, 李世超, 于介江. 2006. *透明矿物鉴定手册*. 北京:地质出版社, 1~258.
- 黄学猛, 张进江, 许志琴. 2016. 电子背散射衍射(EBSD)技术在地球构造变形研究中的应用. *地质学报*, 90(6): 1130~1145.
- 李海龙, 宋传中, 韩建军, 李加好, 任升莲, 张妍, 王微, 杨帆, 李振伟, 王阳阳, 袁芳, 兰瑞烜. 2017. 桐柏杂岩北界剪切带的构造变形特征研究. *地质论评*, 63(3):677~693.
- 秦旭平, 李德威, 刘建雄, 毛晨. 2018. 粤东南燕山期热隆伸展及其古水热系统——以恩平—新丰拆离断层为例. *中国地质*, 45(6): 1188~1204.
- 许志琴, 王勤, 梁风华, 陈方远, 许翠萍. 2009. 电子背散射衍射(EBSD)技术在大陆动力学研究中的应用. *岩石学报*, 1721~1736.

Research advances of microstructural deformation mechanism of feldspar

Baletabieke Bahedaer¹⁾, ZHAO Zhongbao^{* 2,3)}, WANG Genhou¹⁾, SUN Lijing¹⁾, ZHAO Pengbin^{1,4)}

1) *School of Earth Science and Resources, China University of Geosciences, Beijing, 100083;*

2) *Key Laboratory of Deep-Earth Dynamics of Ministry of Natural Resources, Beijing, 100037;*

3) *Institute of Geology, Chinese Academy of Geological Sciences, Beijing, 100037;*

4) *Shaanxi Mineral Resources and Geological Survey, Xi'an, Shaanxi, 710054*

** Corresponding author; zhaozhb04@163.com*

Abstract

Deformation mechanism of rocks, especially microstructure study based on mineral deformation, has long been the study subject of structural geology. From near surface to deep lower crust, the deformation mechanism of felsic rocks convert gradually from brittle fracturing to ductile creep, and the deformation process have been imprinted in rocks in the form of corresponding microstructures. Generally, the deformation mechanism of a kind of mineral, from low temperature-pressure to high temperature-pressure, undergoes continuous transition from micro-cracks to dissolution-precipitation process, to dislocation creep, to dynamic recrystallization, to grain boundary sliding or diffusion creep; and the transition process normally influences or interacts with each other. Feldspars are the most abundant rock-forming minerals in the crust and its deformation behaviors can directly influence crustal rheologies. Therefore, study of micro-deformation mechanism of feldspar is crucial to understanding the properties of crustal rheologies. Feldspars are a unique mineral which consists of mainly two end members: plagioclases and alkali feldspar. The both belongs to different crystal graph system and thus show different deformation behaviors. However, the both can change to each other one under certain temperature-pressure conditions. Hence, the difference of different kind of feldspar in physical and chemical properties makes the feldspar complex in deformation behavior. Begining with micro-deformation mechanism of the rocks, this study described microstructural properties of feldspars, analyzed the performance of feldspar's microstructural deformation under the different temperature conditions, compared the distinction of plagioclases and alkali feldspar, and summarized the influence of different microstructural deformation mechanism on feldspar's CPO. And the study ended with brief introduction to the latest advances of methology and technology used in microstructures.

Key words: Microstructural deformation mechanism; microstructural deformation of feldspar; plagioclase; K-feldspar; crystallographic preferred orientation (CPO)